



PONTIFICIA
**UNIVERSIDAD
CATÓLICA**
DEL PERÚ

th
TECHNISCHE UNIVERSITÄT
ILMENAU

Pontificia Universidad Católica del Perú

Escuela de Posgrado

**ROBUST ESTIMATION OF VERTICAL WHEEL
FORCES VIA MODULATION-BASED SENSOR
FUSION**

**TESIS PARA OPTAR EL GRADO ACADÉMICO DE
MAGÍSTER EN INGENIERÍA DE CONTROL Y
AUTOMATIZACIÓN**

Presentado por: B.Sc. Juan de Dios Segura Rojas

Fecha y Lugar de Nacimiento: 03/09/1993 Lima, Perú

Tutor Responsable (TU ILMENAU): Prof. Dr.-Ing. Johann Reger

Professor Responsable (TU ILMENAU): M. Sc. Matti Noack

Professor Responsable (PUCP): Dr.-Ing. Carlos Gustavo Pérez Zúñiga

Fecha y Lugar: 20/09/2019, Lima



TECHNISCHE UNIVERSITÄT ILMENAU

Department of Computer Science and Automation

Master Thesis

**Robust estimation of vertical wheel forces via
modulation-based sensor fusion**

Submitted by: Juan de Dios Segura Rojas

Date and place of birth: 03. 09. 1993 in Lima, Peru

Course of studies: Technische Kybernetik und Systemtheorie

Supervisor TU-Ilmenau: Prof. Dr.-Ing. Johann Reger

Advisors: M. Sc. Matti Noack

Dr.-Ing. Carlos Gustavo Pérez Zúñiga

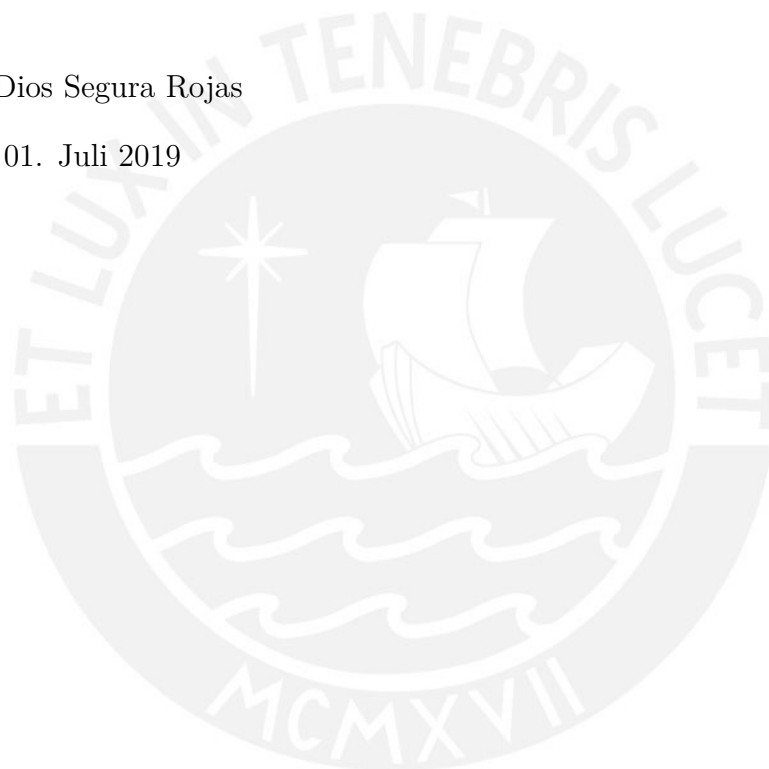
Date of submission: 01. 07. 2019

Erklärung

Ich versichere, dass ich die Arbeit ohne fremde Hilfe und ohne Benutzung anderer als der angegebenen Quellen angefertigt habe und dass die Arbeit in gleicher oder ähnlicher Form noch keiner anderen Prüfungsbehörde vorgelegen hat und von dieser als Teil einer Prüfungsleistung angenommen wurde. Alle Ausführungen, die wörtlich oder sinngemäß übernommen wurden, sind als solche gekennzeichnet.

Juan de Dios Segura Rojas

Ilmenau, 01. Juli 2019



Special thanks

To my parents, for always supporting me despite the distance; to my sisters, for always being a great emotional support; to Dr. Sotomayor and Dr. Pérez from PUCP for the opportunity to study abroad; to my advisor M. Sc. Matti Noack and Prof. Reger of the TU Ilmenau for always being willing to support me academically; to both universities for the quality of education; and to my friends, for being a great source of support and because they have made this stage fun.



Abstract

Since its introduction by Shinbrot, numerous variations of parameter identification based on the Modulating Function Technique (MFT) have been developed. Recently researches have achieved to estimate also states through this method. In this thesis, the MFT is utilized for the estimation, of both parameters and states, that lead to observe the behaviour of the vertical suspension forces on a vehicle over time. In order to deal with the frequency disturbances present by perturbations as measurement noise and vibrations, the Fourier Modulating Function (FMF) as a kernel is proposed. Furthermore, this method is implemented with the concept of sensor fusion. The estimation that results after the implementation of an adaptive observer during the present work is going to show the robustness of the studied technique.

Kurzfassung

Seit der Einführung der Modulationsfunktionstechnik (MFT) durch Shinbrot wurden zahlreiche Methoden zur Identifikation von Parametern entwickelt. Die aktuelle Forschung hat inzwischen auch das Schätzen von Zustandsgrößen mit dieser Technik erreicht. In dieser Masterarbeit wird die MFT für die Zustands- und Parameterschätzung verwendet um das dynamische Verhalten der vertikalen Federung an einem Fahrzeug zu beobachten. Um mit Störungen durch Messrauschen und Vibrationen umzugehen wird die Fouriermodulationsfunktion (FMF) als Kern vorgeschlagen. Des Weiteren wird die Methode mit dem Konzept der Sensorfusion implementiert. Das Ergebnis ist eine robuste Schätzung, wie in der vorliegenden Arbeit gezeigt wird.

Contents

1	Introduction	1
1.1	Motivation	1
1.2	Problem Statement	2
1.3	Objectives	2
2	Modulating Function	4
2.1	Modulating Function Technique	4
2.2	Frequency Domain Modulating Function Approach	6
2.3	Frequency Domain Modulating Function as LMF	8
2.4	Choice of Modulating Function	9
2.4.1	Parameters identification	9
2.4.2	State estimation	11
3	Vehicle Dynamics	12
3.1	Car model	12
3.1.1	Mathematical Relations	12
3.1.2	Variables and parameters	15
4	Adaptive observer	17
5	Simulations	23
5.1	Model Considerations	23
5.2	Implementation	23
5.3	Analysis	25
5.4	Comparison	35
6	Conclusions	37
	List of Figures	39
	List of Tables	40

Bibliography

41



1 Introduction

1.1 Motivation

Estimation of States is an area of great interest on the field of Control Engineering due to the necessity of understanding the complete behaviour of the analysed plant. As is known, there are internal states that cannot be directly determined, either due to the impossibility of carrying out a direct measurement or the high cost of the required measurement systems. A similar problem can be seen when trying to identify parameters, which may not be determined in beforehand. A wide range of identification and estimation methods that solve this problematic have been developed through the years, notwithstanding the complexity of systems can pose a major challenge regarding the design of an observer and can cause great computational cost.

Safety systems of modern terrestrial vehicles are based on reading various sensors, data that can be used for driver monitoring, as well as for automatic steering control, such that dangers like rollover can be avoided. Nevertheless, these sophisticated sensors considerably increase the price of those vehicle.

The content of this thesis is concerned with the design of an adaptive observer for the identification of the necessary readings of Inertial Measurement Units (IMU) and suspension deflection sensors based in the dynamics of a full car model. The method chosen is the MFT based on the Fourier Transform, based on the work of Shinbrot (1957).

The work is structured into six chapters. In the first one, the problem statement, as well as the objectives, are given. The second chapter introduces the necessary definitions and theorems concerning the MFT. Also, the application of these principles for parameters identification and states estimation is explained. In chapter three, the mathematical relations that describe the car model utilised in the investigation are given. In chapter four, the configuration of the employed sensors is presented, and the content of the previous chapters are merged in such a way that an estimator and an

adaptive observer are developed. The model considerations, as well as the implementation of the developed work and the analysis of the results, are presented in chapter five. Finally, the feasibility of using the Modulating Function approach during this work is commented; the contribution of this investigation, some considerations and an outlook on how the work could continue are given.

1.2 Problem Statement

As stated in the previous section, the identification of some states is necessary by means of cheaper sensors. The IMU brings information as the angular rate and accelerations, however, most of the vehicle dynamics depends mathematically on the roll, pitch and yaw angles. The identification of these angles cannot be realised by the means of integration, due to the presence of bias, measurement noise and unknown initial conditions, which causes accumulation of error. Furthermore, the knowledge of some states is necessary to analyse the behaviour of vertical forces that can help to understand the effect of the road on the vehicle. During the present work, the MFT is utilized due to the robustness against noise effect.

1.3 Objectives

This work has as main objective to develop an adaptive observer using the Modulating Function Technique based on the Fourier transform and employing the reading of the aforementioned sensors that can allow to estimate the roll and pitch angles as well as suspension deflection sensors readings that can allow to determine the effect of the vertical forces on a 4-wheel terrestrial vehicle. The following figure outlines the aforementioned:

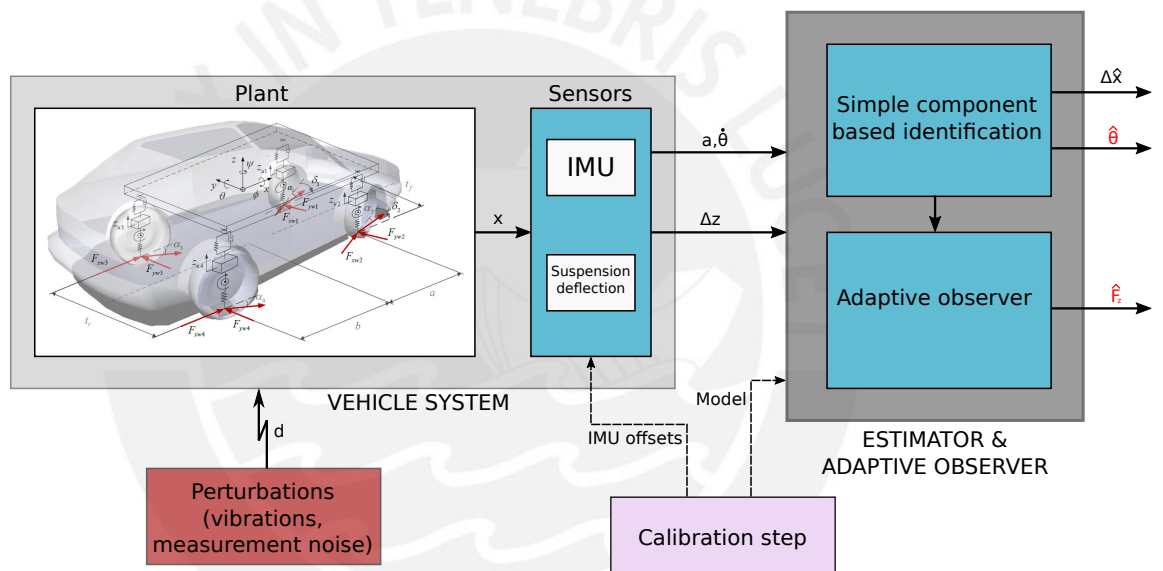


Figure 1.1: Estimation scheme

2 Modulating Function

This chapter begins with a brief historical introduction of the approaches based in the MFT. Then, the mathematical definition of the Modulating Function is given. This is followed by the definition of the Modulation Operator, which allows to transform or 'modulate' a function represented in time domain.

The Frequency Domain Modulating Function approach is introduced and defined in section 2.2 as well as some representations of the components of a MF in this domain. The next section gives an explanation of how to form a Left MF in the frequency domain and the chapter ends with the steps necessary to identify parameters and estimate states using the approach.

2.1 Modulating Function Technique

This technique is an approach based on the work developed by Shinbrot in 1957 with the objective of transforming a differential equation into an algebraic one. Among the different Modulating Functions (MF) developed for parameters identification, Pearson and Lee introduced the FMF in 1985 [PL85], which is based on the frequency domain and is utilised in the present work. Consider the following definitions based on [Shi57].

Definition 2.1 (Modulating Function). *Let $\varphi \in C^{N_d}([0, T] \rightarrow \mathbb{R})$ be a N_d -times continuously differentiable function that for the fixed time horizon $T > 0$ fulfils:*

$$\varphi^{(i)}(0) \cdot \varphi^{(i)}(T) = 0 \quad \forall i \in \{0, 1, \dots, N_d - 1\}.$$

The MF φ of order N_d is called

(i) Total Modulating Function (TMF) if

$$\varphi^{(i)}(0) = \varphi^{(i)}(T) = 0 \quad \forall i \in \{0, 1, \dots, N_d - 1\},$$

(ii) *Left Modulating Function (LMF) if*

$$\varphi^{(i)}(0) = 0, \varphi^{(i)}(T) \neq 0 \quad \forall i \in \{0, 1, \dots, N_d - 1\},$$

(iii) *Right Modulating Function (RMF) if*

$$\varphi^{(i)}(0) \neq 0, \varphi^{(i)}(T) = 0 \quad \forall i \in \{0, 1, \dots, N_d - 1\}.$$

Remark. It is important to consider that the integration horizon T represents a moving horizon that maintains its length. So for any time t , the horizon will be defined as $[t - T, t]$.

Definition 2.2 (Modulation operator). *Let $f : [t - T, t] \rightarrow \mathbb{R}$ be an integrable time function, with $t \in \mathbb{R}$, $T > 0$ and the MF $\varphi \in C^{N_d}([0, T] \rightarrow \mathbb{R})$. The Modulation operator is defined for f under the MF φ as*

$$L^i[f] := \int_{t-T}^t (-1)^i \varphi^{(i)}(\tau - t + T) f(\tau) d\tau \quad (2.1)$$

The modulation operator abbreviates the integral transformation with respect to the moving horizon $[t - T, T]$, where the MF acts as the kernel.

If in (2.1) f is replaced by its i -th derivative:

$$L^0[f^{(i)}] := \int_{t-T}^t \varphi(\tau - t + T) f^{(i)}(\tau) d\tau \quad (2.2)$$

Theorem 2.1. *Let $f : [t - T, t] \rightarrow \mathbb{R}$ be an integrable time function, with $t \in \mathbb{R}$, $T > 0$ and TMF $\varphi \in C^{N_d}$ be a TMF. Then*

$$L^i[f] \equiv L^0[f^{(i)}]. \quad (2.3)$$

Proof. The operator $L^0[f^{(i)}]$ can be expanded through the concept of repeated integration by parts, which will be considered for the period from 0 to T for simplicity:

$$L^0[f^{(i)}] = \left[\varphi(\tau) f^{(i-1)} \Big|_0^T + \dots + (-1)^{i-1} \varphi^{(i-1)}(\tau) f \Big|_0^T + (-1)^i \int_0^T \varphi^{(i)}(\tau) f d\tau \right] \quad (2.4)$$

Considering the boundary conditions defined for the TMF:

$$L^0[f^{(i)}] = (-1)^i \int_0^T \varphi^{(i)}(\tau) f(\tau) d\tau$$

□

Remark. The modulating operator represents an integration, so it can be assumed that the same properties of this operator are fulfilled for $L^i[f]$.

An advantage that results of using this method is that the calculation of derivative terms is avoided, the derivatives are transferred to the MF as proved.

2.2 Frequency Domain Modulating Function Approach

In addition to the MF with trigonometric or polynomial structure, which are commonly used, Pearson, Lee, Unbehauen et al. also developed frequency approaches, which were unified by [ART14] into the representation called Frequency Domain Modulating Function (FDMF). These MF are based on the Hartley and Fourier Transform. In the present work the latter one will be utilized, and from now on the MF based on it will be denominated as FMF. The FMF has been chosen due to its filtering properties against the noise as explained by [Agu14].

The Fourier Transform has a structure very similar to the one defined on (2.1). The representation that fits better is defined below.

Definition 2.3 (Finite Fourier Transform). *Let $f : [t - T, t] \rightarrow \mathbb{R}$ be an integrable function, with $t \in \mathbb{R}$ and $T > 0$. The Finite Fourier Transform is defined as*

$$\mathcal{F}(k\omega) = \frac{1}{T} \int_{t-T}^t f(\tau) e^{-jk\omega(\tau-t+T)} d\tau,$$

where $\omega = \frac{2\pi}{T}$ and $k \in \mathbb{Z}$.

Following the similarity with (2.1) mentioned before, the chosen kernel is $\Psi(\boldsymbol{\omega}, t) = e^{-j\boldsymbol{\omega}t}$, where $\boldsymbol{\omega} = [\omega_1, \dots, \omega_{N_\omega}]^\top$ is a vector of N_ω multiples of ω , so

$$\Psi(\boldsymbol{\omega}, t) = e^{-j\boldsymbol{\omega}t} = [e^{-j\omega_1 t}, \dots, e^{-j\omega_{N_\omega} t}]^\top \quad (2.5)$$

If a right linear combination matrix $R_m \in \mathbb{R}^{(N_\omega - N_d) \times N_\omega}$ is determined as will be

shown later, a MF with the structure $\varphi(t) = \frac{1}{T}R_m\Psi(\boldsymbol{\omega}, t)$ can be obtained, with $\Psi(\boldsymbol{\omega}, t) \in \mathbb{R}^{N_\omega}$.

Theorem 2.2. *Let $f : [t - T, t] \rightarrow \mathbb{R}$ be an integrable time function, with $t \in \mathbb{R}$, $T > 0$. The modulation operator has the form*

$$L^i[f] := R_m D_i(\boldsymbol{\omega}) \mathcal{F}(k\boldsymbol{\omega})$$

where D_i follows from the time derivative of the kernel $\Psi(\boldsymbol{\omega}, t)$.

Proof. Replacing the structure defined for $\varphi(t)$ in (2.1) gives

$$L^i[f] := \frac{1}{T}(-1)^i R_m \int_{t-T}^t \Psi^{(i)}(\boldsymbol{\omega}, \tau - t + T) f(\tau) d\tau. \quad (2.6)$$

where the derivative of the kernel has the structure $\Psi^{(i)}(\boldsymbol{\omega}, t) = (-1)^i D_i(\boldsymbol{\omega}) \Psi(\boldsymbol{\omega}, t)$, or

$$\Psi^{(i)}(\boldsymbol{\omega}, t) := (-1)^i (j)^i \underbrace{\begin{bmatrix} \omega_1 & & & \\ & \omega_2 & & \\ & & \ddots & \\ & & & \omega_{N_\omega} \end{bmatrix}}_{D_i(\boldsymbol{\omega})} \underbrace{\begin{bmatrix} e^{-j\omega_1 t} \\ e^{-j\omega_2 t} \\ \vdots \\ e^{-j\omega_{N_\omega} t} \end{bmatrix}}_{\Psi(\boldsymbol{\omega}, t)}.$$

Then, replacing and reordering the terms in (2.6) gives

$$L^i[f] := R_m D_i(\boldsymbol{\omega}) \frac{1}{T} \int_{t-T}^t f(\tau) e^{-j\boldsymbol{\omega}t} d\tau = R_m D_i(\boldsymbol{\omega}) \mathcal{F}(k\boldsymbol{\omega}) \quad (2.7)$$

□

For a TMF, the equivalence (2.3) is fulfilled.

The kernel $\Psi(\boldsymbol{\omega}, t)$ can not be 0, it does not matter the value of t . That is why it is necessary to determine the combination matrix R_m . For its calculation, the structure of the FDMF after (2.5) is given:

$$\varphi(t) = [\varphi_1(t), \dots, \varphi_{N_\omega - N_d}(t)]^\top \quad (2.8)$$

or $\varphi(t) = R_m [\Psi(\omega_1, t), \dots, \Psi(\omega_{N_\omega}, t)]^\top$. This structure can be reshaped, so it includes its derivatives. Also the boundary conditions for a TMF seen in Definition 2.1 are

considered. Then, (2.8) evaluated on T has the form:

$$[\varphi(T), \varphi^{(1)}(T), \dots, \varphi^{(N_d-1)}(T)]^\top = [\Psi(\boldsymbol{\omega}, T), \Psi^{(1)}(\boldsymbol{\omega}, T), \dots, \Psi^{N_d-1}(\boldsymbol{\omega}, T)]^\top R_m^\top. \quad (2.9)$$

This last representation can be rewritten as MR_m^\top . Due to the aforementioned boundary conditions, (2.9) can be evaluated at 0. Finally, R_m is calculated as the transpose of the null space of M .

2.3 Frequency Domain Modulating Function as LMF

In (2.5) the structure of the kernel is conformed by elements with the shape $e^{-j(k\omega)t}$ for $k \in \{1, \dots, N_w\}$. If this kernel is evaluated on the integration limits, one gets

$$e^{-j(k\omega)T} = e^{-j(k\frac{2\pi}{T})T} = e^{-j2\pi k} = 1 = e^{-j(k\omega)0}, \quad (2.10)$$

and can be noticed that the boundary conditions for a LMF can not be met, i.e if $\varphi(T) = 0 \rightarrow \varphi(0) = 0$.

It can be concluded that a LMF based purely on the structure of Fourier Transform cannot be obtained. In [Web17] a LMF is given, which keeps the properties of the defined kernel. It has the structure of the TMF kernel extending it by a polynomial term and fulfils the boundary conditions. Then, the new LMF is

$$\varphi(t) = \frac{1}{T} R_m \Psi(\boldsymbol{\omega}, t) t^{N_d} \quad (2.11)$$

The equivalence (2.3) was defined due to the effect of the boundary conditions of a TMF on equation (2.4). Analogously, for a LMF the boundary conditions must be fulfilled, so in this case:

$$\begin{aligned} L^0[f^{(i)}] &= \\ &= \left[\varphi(T) f^{(i-1)}(t) + \dots + (-1)^{i-1} \varphi^{(i-1)}(T) f(t) + (-1)^i \int_{t-T}^t \varphi^{(i)}(\tau - t + T) f(\tau) d\tau \right] \end{aligned} \quad (2.12)$$

And can be simplified using also the equation (2.7) to get the structure

$$\begin{aligned} L^0[f^{(i)}] &= \sum_{k=1}^i (-1)^{k-1} \varphi^{(k-1)}(T) f^{(i-k)}(t) + R_m D_i(\omega) \mathcal{F}(k\omega) \\ &= \sum_{k=1}^i (-1)^{k-1} \varphi^{(k-1)}(T) f^{(i-k)}(t) + L^i[f] \end{aligned} \quad (2.13)$$

R_m is determined similar to (2.9) with the consideration that the null space of M must be evaluated only in $t = 0$. Due to this boundary condition, the LMF and its derivatives are continuously growing over time as seen in Figure (5.7). The number of frequencies N_w and the horizon T have to be chosen carefully to obtain a coherent maximum value for φ .

2.4 Choice of Modulating Function

Choosing which kind of MF among the ones defined at the beginning of this chapter depends mainly on what one needs to calculate. During this work, only the TMF and the LMF are used for parameter identification and state estimation respectively.

The following equation

$$y^{(n)} + a_{n-1}y^{(n-1)} + \dots + a_0y = b_{n-2}u^{(n-2)} + \dots + b_0u, \quad (2.14)$$

represents a SISO system. It will be used to give a better understanding of the following subsections.

2.4.1 Parameters identification

For parameters identification, one choose the TMF. The boundary conditions of this kind of MF can be interpreted as the unnecessariness of information storing. Also, the equivalence (2.3) allows to avoid derivatives calculation. Following the example (2.14), the whole differential equation is multiplied by $\varphi(t)$ and integrated over the horizon:

$$L^n[y] + a_{n-1}L^{n-1}[y] + \dots + a_0L^0[y] = b_{n-2}L^{n-2}[u] + \dots + b_0L^0[u] \quad (2.15)$$

Equation (2.15) can be rearranged into the form $z = \eta^\top \theta$, where η represents the regressor and θ is the parameter vector:

$$\underbrace{L^n[y]}_z = \underbrace{\left(-L^{n-1}[y] \quad \dots \quad -L^0[y] \quad L^{n-2}[u] \quad \dots \quad L^0[u] \right)}_{\eta^\top} \underbrace{\begin{pmatrix} a_{n-1} \\ \vdots \\ a_0 \\ b_{n-2} \\ \vdots \\ b_0 \end{pmatrix}}_{\theta} \quad (2.16)$$

A classical online parameter estimation algorithm is the gradient method:

$$\dot{\hat{\theta}} := \frac{\partial J}{\partial \hat{\theta}} = -\eta(\eta^\top \hat{\theta} - z), \quad (2.17)$$

where $J(\hat{\theta}) = \frac{1}{2} (\eta^\top \hat{\theta} - z)^\top (\eta^\top \hat{\theta} - z)$ is the cost function. To get $\hat{\theta}$, (2.17) has to be integrated over runtime. A nonlinear gradient method and an extended form can be found in [NRERM16].

The parameters can also be estimated using a simple inversion based approach. Utilising as many MF as number of parameter to estimate, a well posed system of linear equations can be obtained. For $n = 2$:

$$\underbrace{\begin{pmatrix} L_1^2[y] \\ L_2^2[y] \\ L_3^2[y] \end{pmatrix}}_z = \underbrace{\begin{pmatrix} -L_1^1[y] & -L_1^0[y] & L_1^0[u] \\ -L_2^1[y] & -L_2^0[y] & L_2^0[u] \\ -L_3^1[y] & -L_3^0[y] & L_3^0[u] \end{pmatrix}}_{\eta^\top} \underbrace{\begin{pmatrix} a_1 \\ a_0 \\ b_0 \end{pmatrix}}_{\theta}$$

Then, the parameter vector is estimated:

$$\hat{\theta}(t) = (\eta \eta^\top)^{-1} \eta \quad z, \quad (2.18)$$

which needs η to be full row rank.

2.4.2 State estimation

Once the parameters are identified, the states can be reconstructed utilising the LMF, whose boundary conditions allow to observe the evolution of a state over time. For (2.14) with $n = 2$, the differential equation is multiplied by φ and integrated over the horizon:

$$\varphi(T)\dot{y}(t) - \dot{\varphi}(T)y(t) + L^2[y] + a_1(\varphi(T)y(t) + L^1[y]) + a_0L^0[y] = b_0L^0[u] \quad (2.19)$$

This equation can be rearranged so the states are isolated (based on [NBH⁺18]):

$$\underbrace{L^2[y] + a_1L^1[y] + a_0L^0[y] - b_0L^0[u]}_q = \underbrace{(\dot{\varphi}(T) - a_1\varphi(T) \quad -\varphi(T))}_\delta \underbrace{\begin{pmatrix} y(t) \\ \dot{y}(t) \end{pmatrix}}_{x(t)} \quad (2.20)$$

The resulting equation $q = \delta x(t)$ is augmented by as many distinct MF φ_i as the number of states to estimate. Following the example:

$$\underbrace{\begin{pmatrix} L_1^2[y] + a_1L_1^1[y] + a_0L_1^0[y] - b_0L_1^0[u] \\ L_2^2[y] + a_1L_2^1[y] + a_0L_2^0[y] - b_0L_2^0[u] \end{pmatrix}}_Q = \underbrace{\begin{pmatrix} \dot{\varphi}_1(T) - a_1\varphi_1(T) & -\varphi_1(T) \\ \dot{\varphi}_2(T) - a_1\varphi_2(T) & -\varphi_2(T) \end{pmatrix}}_\Delta \underbrace{\begin{pmatrix} y(t) \\ \dot{y}(t) \end{pmatrix}}_{x(t)}$$

It can be noticed that Δ is constant and can be computed offline. Using least squares, the states are reconstructed:

$$\hat{x}(t) = (\Delta^\top \Delta)^{-1} \Delta^\top Q \quad (2.21)$$

In this chapter, the necessary knowledge for the development of this work is explained. Also, an offline method to observe states using the MFT is given. For parameter identification, an online estimator that uses the gradient method, as well as an offline method based on a simple inversion, are explained. The former is implemented during this work.

3 Vehicle Dynamics

The present chapter begins with a brief explanation of the chosen car model, as well as the importance of it. Then, mathematical relations that group the vehicle dynamics are given.

3.1 Car model

The most important requirement for the investigation of vehicle motion is an appropriate model of the vehicle dynamics. The number of Degrees of Freedom (DoF) of the model varies from the classic 'bicycle model' up to more realistic models, whose complexity implies a higher number of differential equations. Choosing the right model allows to understand the behaviour of the vehicle according to the properties that one wants to analyse. This can be for example the applied forces, suspension or rotational accelerations.

The following 14 DoF vehicle model based on [SWSI13] is given, in which the motion in space of the vehicle body has six degrees of freedom (longitudinal, lateral, vertical, roll, pitch and yaw motions).

3.1.1 Mathematical Relations

The following relations are based on the works of [Ell94], [SSS09] and [NBH⁺18]. Using the described model in figure 3.1 as a reference, the displacement of sprung mass on the vertical axis is defined by:

$$m_s \cdot \ddot{z}_{cg} = \sum_{i=1}^4 F_{si} \quad (3.1)$$

where m_s represents the mass of the sprung and \ddot{z}_{cg} is the vertical acceleration of the body evaluated on its center of gravity (COG) without considering the effect of the gravitational force. The forces F_{si} are the result of combining the spring and damper

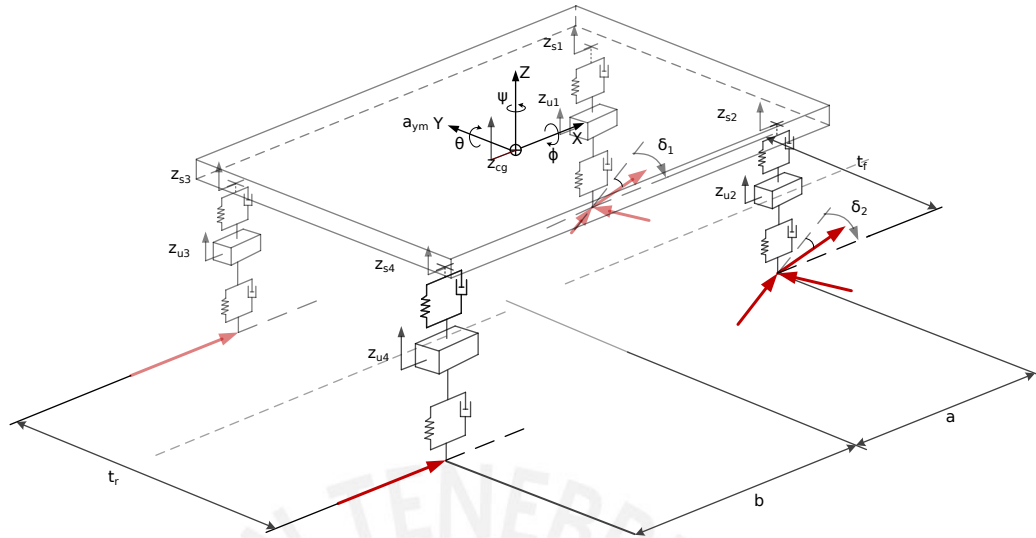


Figure 3.1: 14 DOF vehicle model

forces (i is 1 for the front left, 2 for the front right, 3 for the rear left and 4 for the rear right).

$$F_{si} = \underbrace{K_{si}(z_{ui} - z_{si})}_{\text{Spring force}} + \underbrace{C_{si}(\dot{z}_{ui} - \dot{z}_{si})}_{\text{Damper force}} \quad (3.2)$$

where z_{ui} and z_{si} represent the position on the Z-axis of the unsprung and sprung of each of the 4 corners respectively. K_{si} is the vertical stiffness coefficient of the respective suspension and C_{si} represents the vertical damping coefficient of each suspension. Through the principle of the balance of moments, the pitch effect of the vehicle is given by:

$$I_{\theta}\ddot{\theta} = -(F_{s1} + F_{s2})a + (F_{s3} + F_{s4})b \quad (3.3)$$

where I_{θ} is the moment of inertia around the pitch axis, $\ddot{\theta}$ is the pitch acceleration, a is the distance from the COG to the front axle and b is the distance from the COG to the back axle. Similarly, the roll effect of the vehicle is represented by:

$$I_{\phi}\ddot{\phi} = (F_{s1} - F_{s2})\frac{T_f}{2} + (F_{s3} - F_{s4})\frac{T_r}{2} \quad (3.4)$$

where I_{ϕ} is the moment of inertia about roll axis, $\ddot{\phi}$ is the roll acceleration, T_f is the length of the front track and T_r is the length of the back track.

The equation of body roll motion, taken from [HBM04], is:

$$I_\phi \ddot{\phi} + C_\phi \dot{\phi} + K_\phi \phi = -m_s a_{ym} h_{roll} \quad (3.5)$$

where K_ϕ is the combined roll stiffness of suspension and tires, C_ϕ is the combined roll damping of suspension and tires and a_{ym} is the measured lateral acceleration. Equation (3.5) simplifies the calculation of a_{ym} , which can be compensated with the effect of the gravity and the roll angle to obtain the acceleration in the Y-axis.

The following geometric relations allow to relate the corner dynamics to the rotational angles:

$$\begin{aligned} z_{s1} &= z_{cg} - a \sin \theta + \frac{t_f}{2} \sin \phi, \\ z_{s2} &= z_{cg} - a \sin \theta - \frac{t_f}{2} \sin \phi, \\ z_{s3} &= z_{cg} + b \sin \theta + \frac{t_r}{2} \sin \phi, \\ z_{s4} &= z_{cg} + b \sin \theta - \frac{t_r}{2} \sin \phi \end{aligned} \quad (3.6)$$

Throughout the present work, a small pitch angle is considered. This assumption is valid due to the linear behaviour of the sine at small angles. Then, relations in (3.6) have the form:

$$\begin{aligned} z_{s1} &= z_{cg} - a\theta + \frac{t_f}{2} \sin \phi, \\ z_{s2} &= z_{cg} - a\theta - \frac{t_f}{2} \sin \phi, \\ z_{s3} &= z_{cg} + b\theta + \frac{t_r}{2} \sin \phi, \\ z_{s4} &= z_{cg} + b\theta - \frac{t_r}{2} \sin \phi \end{aligned} \quad (3.7)$$

A last important dynamic component related with the mass of the suspension (or unsprung mass) is the unknown road input. The relation with respect to the suspension deflection, and que position of the sprung is given:

$$m_{ui} \ddot{z}_{ui} = -k_{si}(z_{ui} - z_{si}) - C_{si}(\dot{z}_{ui} - \dot{z}_{si}) - k_{ui}(z_{ui} - \mathbf{u}_i) - c_{ui}(\dot{z}_{ui} - \dot{\mathbf{u}}_i) \quad (3.8)$$

As the wheel damping coefficient is very small compared with the other coefficients, the component $c_{ui}(\dot{z}_{ui} - \dot{\mathbf{u}}_i)$ seen in (3.8) can be ignored.

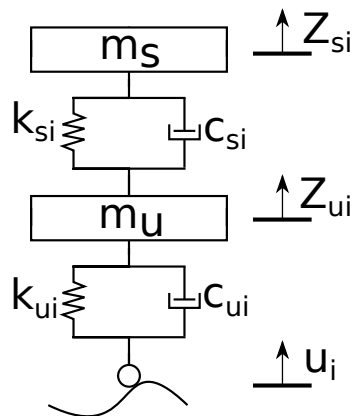


Figure 3.2: 1 DOF vehicle model

3.1.2 Variables and parameters

The following table gives a summary of the variables defined so far:

Variable	Description
z_{cg}	Vertical position of COG
z_{s1}	Vertical position of front left sprung mass corner
z_{s2}	Vertical position of front right sprung mass corner
z_{s3}	Vertical position of rear left sprung mass corner
z_{s4}	Vertical position of rear right sprung mass corner
z_{u1}	Vertical position of front left unprung mass
z_{u2}	Vertical position of front right unprung mass
z_{u3}	Vertical position of rear left unprung mass
z_{u4}	Vertical position of rear right unprung mass
u_1	Road profile input in the front left wheel
u_2	Road profile input in the front right wheel
u_3	Road profile input in the rear left wheel
u_4	Road profile input in the rear right wheel
θ	Vehicle pitch angle
ϕ	Vehicle roll angle

Table 3.1: Described variables

The used parameters during this work where obtained from a Range Rover model on CarMaker® shared by the Automotive Engineering Group, TU Ilmenau:

Parameter	description	Value
m_s	Sprung mass weight	1661.95 kg
m_u	Unsprung mass weight	425.45 kg
a	Distance from COG to front axle	1.0365 m
b	Distance from COG to rear axle	1.6255 m
t_f	Front track	1.616 m
t_r	Rear track	1.613 m
h_{cog}	Heigh of COG	0.634 m
$K_{s1,2}$	Suspension's vertical stiffness coefficient (front)	$2.5 \cdot 10^4 \text{N/m}$
$K_{s3,4}$	Suspension's vertical stiffness coefficient (rear)	$3 \cdot 10^4 \text{N/m}$
K_{ui}	Wheel stiffness coefficient	$7.5 \cdot 10^4 \text{N/m}$
$C_{s1,2}$	Suspension's vertical damping coefficient (front)	$1.5 \cdot 10^3 \text{N s/m}$
$C_{s3,4}$	Suspension's vertical damping coefficient (rear)	$1.5 \cdot 10^3 \text{N s/m}$
K_ϕ	Combined roll stiffness of suspension and tires	900 N m/rad
C_ϕ	Combined roll damping of suspension and tires	60 Nm/(rad s)
I_θ	Moment of inertia along pitch axis	3481.172 kg m ²
I_ϕ	Moment of inertia along roll axis	912.124 kg m ²

Table 3.2: Technical parameters

4 Adaptive observer

In this chapter, the algorithms for recursive joint estimation of parameters and states are developed. These elements will compose what here is defined as an adaptive observer.

On Table 3.2, some parameters like vertical stiffness coefficients and vertical damping coefficients are given. As any mechanical structure, gradual wear out over time inevitably happens due to both internal and external factors. In consequence, their parameters are altered slowly. Accurate information is necessary, so a calibration step is fundamental before the development of an observer or any control structure. For this purpose, the MFT will be used together with the readings of 5 IMUs and 4 suspension deflection sensors. A scheme based on the full car model given in figure 4.1 shows the distribution of the IMUs (represented in red) in each corner of the vehicle and in its COG, as well as the suspension deflection sensors (represented in green):

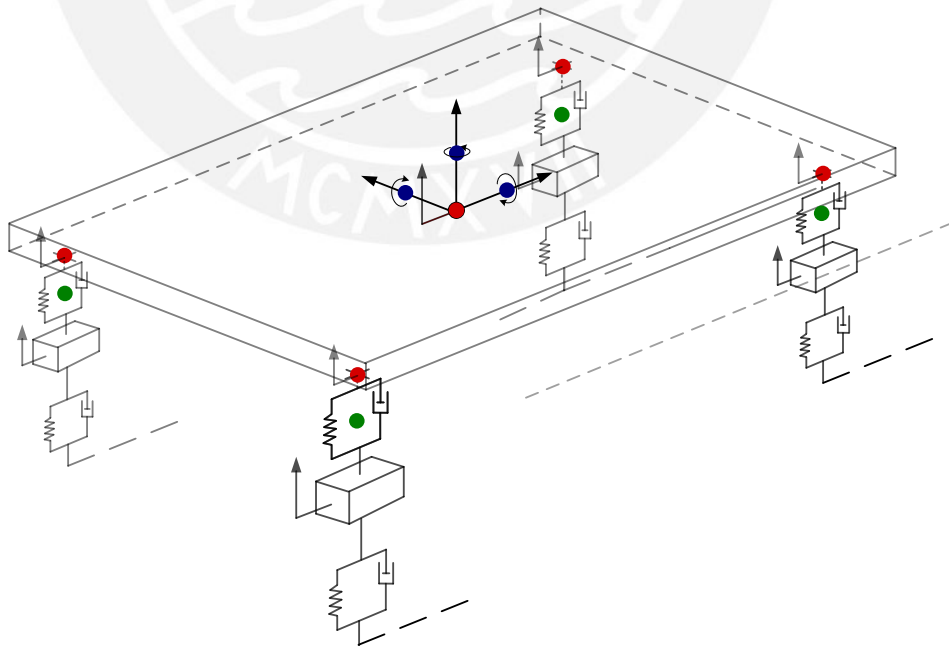


Figure 4.1: Sensors configuration

The following readings from the sensors are obtained:

$$Y = \begin{pmatrix} a_{ym} + b_y \\ \ddot{z}_{cg} + b_z \\ \ddot{z}_{s1} + b_1 \\ \ddot{z}_{s2} + b_2 \\ \ddot{z}_{s3} + b_3 \\ \ddot{z}_{s4} + b_4 \\ \Delta z_1 + b_{\Delta 1} \\ \Delta z_2 + b_{\Delta 2} \\ \Delta z_3 + b_{\Delta 3} \\ \Delta z_4 + b_{\Delta 4} \\ \dot{\theta} + b_{\theta} \\ \dot{\phi} + b_{\phi} \end{pmatrix} + \eta(t) = \begin{pmatrix} y_y \\ y_z \\ y_1 \\ y_2 \\ y_3 \\ y_4 \\ \Delta y_1 \\ \Delta y_2 \\ \Delta y_3 \\ \Delta y_4 \\ y_{\dot{\theta}} \\ y_{\dot{\phi}} \end{pmatrix} \quad (4.1)$$

where Δz_i is $z_{ui} - z_{si}$, b is the respective bias and $\eta(t)$ represents the reading noise. The vertical displacement of the sprung mass is obtained replacing (3.2) in (3.1):

$$m_s \cdot \ddot{z}_{cg} = \sum_{i=1}^4 (K_{si} \Delta z_i + C_{si} \Delta \dot{z}_i) \quad (4.2)$$

and can be rewritten in a way that only depends on the outputs and the bias:

$$m_s \cdot (y_z - b) = \sum_{i=1}^4 [K_{si} (\Delta y_i - b_{\Delta i}) + C_{si} \Delta \dot{y}_i] \quad (4.3)$$

For this first step, as parameters are to be determined, a TMF is used as explained in subsection 2.4.1. As a result, the following equation is obtained:

$$L^1[y_z] = \begin{pmatrix} L^1[\Delta y_1] & L^2[\Delta y_1] & \dots & L^1[\Delta y_4] & L^2[\Delta y_4] \end{pmatrix} \begin{pmatrix} \frac{K_{s1}}{m_s} \\ \frac{C_{s1}}{m_s} \\ \vdots \\ \frac{K_{s4}}{m_s} \\ \frac{C_{s4}}{m_s} \end{pmatrix} \quad (4.4)$$

As can be seen, the bias effect is not considered any more. This happens because it does not change over time, so it is compensated, i.e, it is multiplied by $\varphi^{(n)}(t) - \varphi^{(n)}(t - T)$, which gives 0 due to the boundary conditions of the TMF.

Remark. Instead of multiplying for $\varphi(t)$ one can choose a derivative of this MF, but it will increase the computational cost.

The maximum derivative order of φ can be reduced by 1 if $\Phi(0) = \Phi(T) = 0$, with $\dot{\Phi} = \varphi$, is guaranteed as proposed by [NBH⁺18]. From the equation of body roll motion seen in (3.5), the second derivative of a MF φ is used due to the presence of the unknown roll angle ϕ . This will allow to express it in function of its derivative:

$$\begin{aligned} \int_{t-T}^t \ddot{\varphi}(\tau - t + T)\phi(\tau)d\tau &= - \int_{t-T}^t \dot{\varphi}(\tau - t + T)\dot{\phi}(\tau)d\tau \\ &= - \int_{t-T}^t \dot{\varphi}(\tau - t + T)y_{\dot{\phi}}d\tau \\ &= L^1[y_{\dot{\phi}}] \end{aligned} \quad (4.5)$$

So the modulated equation is obtained:

$$I_{\phi}L^3[y_{\dot{\phi}}] + C_{\phi}L^2[y_{\dot{\phi}}] + K_{\phi}L^1[y_{\dot{\phi}}] = -m_s h_{roll}L^2[y_y], \quad (4.6)$$

which is rearranged:

$$-L^2[y_y] = \begin{pmatrix} L^3[y_{\dot{\phi}}] & L^2[y_{\dot{\phi}}] & L^1[y_{\dot{\phi}}] \end{pmatrix} \begin{pmatrix} \frac{I_{\phi}}{m_s \cdot h_{roll}} \\ \frac{C_{\phi}}{m_s \cdot h_{roll}} \\ \frac{K_{\phi}}{m_s \cdot h_{roll}} \end{pmatrix} \quad (4.7)$$

Following a similar process using relations seen in (3.7), one can take directly the second derivative, e.g:

$$\ddot{z}_{s1} = \ddot{z}_{cg} - a\ddot{\theta} + \frac{t_f}{2} \left(\frac{\partial^2 \sin \phi}{\partial t^2} \right) \quad (4.8)$$

and then represent it in function of the sensors readings:

$$y_1 - b_1 = y_z - b_2 - a\dot{y}_{\theta} + \frac{t_f}{2} \left(\frac{\partial^2 \sin \phi}{\partial t^2} \right) \quad (4.9)$$

which can be modulated as in (4.4). This gives:

$$-L^1[y_1] = -L^1[y_z] + aL^2[y_{\dot{\theta}}] - \frac{t_f}{2}L^3[\sin \phi] \quad (4.10)$$

And consequently, the other relations are modulated in the same manner. After iso-

lating the desired parameters:

$$\begin{aligned} \begin{pmatrix} L^1[y_z - y_1] \\ L^1[y_z - y_2] \end{pmatrix} &= \begin{pmatrix} L^2[y_{\dot{\theta}}] & -L^3[\sin \phi] \\ L^2[y_{\dot{\theta}}] & L^3[\sin \phi] \end{pmatrix} \begin{pmatrix} a \\ \frac{t_f}{2} \end{pmatrix} \\ \begin{pmatrix} L^1[y_z - y_3] \\ L^1[y_z - y_4] \end{pmatrix} &= \begin{pmatrix} -L^2[y_{\dot{\theta}}] & -L^3[\sin \phi] \\ -L^2[y_{\dot{\theta}}] & L^3[\sin \phi] \end{pmatrix} \begin{pmatrix} b \\ \frac{t_r}{2} \end{pmatrix} \end{aligned} \quad (4.11)$$

One can notice that the roll angle ϕ is needed to be known for the modulation. Theoretically, it can be calculated by integrating the roll rate $y_{\dot{\phi}}$ that was measured by the IMU; however, the presence of bias, the measurement noise as well as unknown initial conditions cause large calculation error. The roll angle will be estimated later during this work. Its estimation does not depend on the parameters identified in (4.11).

Among the sensors, the suspension deflection ones always need to be set to zero, this due to the dependence of the load distribution to set their initial condition.

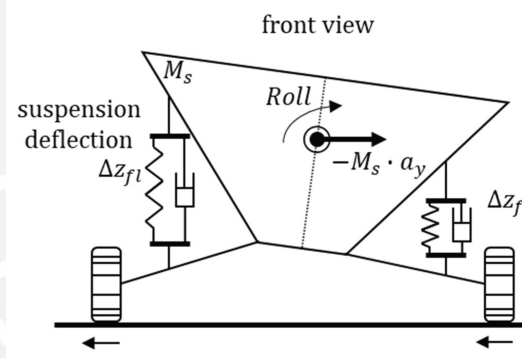


Figure 4.2: Example of initial condition of suspension deflection sensors [NPL⁺18]

Equation (4.3) can be modified, so instead it can depend of the derivative of the state instead of the output:

$$m_s \cdot (y_z - b) = \sum_{i=1}^4 [K_{si}(\Delta y_i - b_{\Delta i}) + C_{si}(\dot{z}_{ui} - \dot{z}_{si})], \quad (4.12)$$

as one needs to estimate the state, a LMF is utilized. This gives:

$$m_s \left(-L^1[y_z] - \varphi(T)b_z \right) = \sum_{i=1}^4 \left[K_{si} \left(-L^1[\Delta y_i] - \varphi(T)b_{\Delta i} \right) + C_{si} \left(\dot{\varphi}(T)(\Delta z_i) - L^2[\Delta z_i] \right) \right] \quad (4.13)$$

The number of necessary modulations is reduced thanks to the properties of the definite

integrals. Equation (4.13) is then restructured as follows:

$$L^1 \left[-m_s y_z + \sum_{i=1}^4 K_{si} \Delta y_i \right] + L^2 \left[\sum_{i=1}^4 C_{si} \Delta y_i \right] = m_s \varphi(T) b_z + \sum_{i=1}^4 [(C_{si} \dot{\varphi}(T) - K_{si} \varphi(T)) b_{\Delta i} + C_{si} \dot{\varphi}(T) \Delta z_i] \quad (4.14)$$

Now, following least squares as shown in (2.21), estimation of the bias of the vertical acceleration read by the IMU in the COG and the states Δz_i with their respective bias can be performed. This allows the calibration of the suspension deflection sensors. It is important to notice that to perform the estimation seen in (4.14) it is necessary the use of 9 different MF. A similar procedure can be realized with decoupled relations as (3.3) or (3.4), thus the four bias $b_{\Delta i}$ can be estimated in a previous step, what will allow to reduce to 5 the number of different MF needed in (4.14).

As was explained in the previous section, roll and pitch angles have to be estimated. For the former, body roll motion equation described in (3.5) is used. This time, the equivalence (4.5) cannot be used due to the necessity of using a LMF for this step. Instead, the boundary conditions allow to express the modulation of ϕ as a function of the output, its bias and the angle itself:

$$\begin{aligned} \int_{t-T}^t \ddot{\varphi}(\tau - t + T) \phi(\tau) d\tau &= \dot{\varphi}(T) \phi(t) - \int_{t-T}^t \dot{\varphi}(\tau - t + T) \dot{\phi}(\tau) d\tau \\ &= \dot{\varphi}(T) \phi(t) - \int_{t-T}^t \dot{\varphi}(\tau - t + T) [y_{\dot{\phi}} - b_{\phi}] d\tau \\ &= \dot{\varphi}(T) \phi(t) + L^1[y_{\dot{\phi}}] + \phi(T) b_{\phi} \end{aligned} \quad (4.15)$$

After modulating, one gets:

$$\begin{aligned} I_{\phi} \left(\ddot{\varphi}(T) y_{\dot{\phi}} + L^3[y_{\dot{\phi}}] \right) + C_{\phi} \left(L^2[y_{\dot{\phi}}] - \dot{\varphi}(T) b_{\phi} \right) + K_{\phi} \left(\dot{\varphi}(T) \phi(t) + L^1[y_{\dot{\phi}}] + \varphi(T) b_{\phi} \right) \\ = -m_s h_{roll} (L^2[y_y] - \dot{\varphi}(T) b_y) \end{aligned} \quad (4.16)$$

and can be regrouped as follows:

$$\begin{aligned}
& I_\phi L^3[y_{\dot{\phi}}] + L^2[C_\phi y_{\dot{\phi}} + m_s h_{roll} y_y] + K_\phi L^1[y_{\dot{\phi}}] = \\
& = \begin{pmatrix} -I_\phi \ddot{\varphi}(T) & -K_\phi \dot{\varphi}(T) & m_s h_{roll} \dot{\varphi}(T) & C_\phi \dot{\varphi}(T) - K_\phi \varphi(T) \end{pmatrix} \begin{pmatrix} y_{\dot{\phi}} \\ \phi(t) \\ b_y \\ b_\phi \end{pmatrix} \quad (4.17)
\end{aligned}$$

On a similar manner, the pitch angle θ can be estimated using the geometric relation seen in (3.7) and using $\ddot{\varphi}$ as a LMF. Following the same process as before only for the first geometric relation (front left), one gets:

$$\begin{aligned}
& L^1[y_1] - L^1[y_z] + aL^2[y_{\dot{\theta}}] - \frac{t_f}{2} L^3[\sin \phi] = \\
& = \begin{pmatrix} \ddot{\varphi}(T) & -\dot{\varphi}(T) & a\ddot{\varphi}(T) & -\varphi(T) & \varphi(T) & a\dot{\varphi}(T) \end{pmatrix} \begin{pmatrix} z_{s1} - z_{cg} \\ \dot{z}_{s1} - \dot{z}_{cg} \\ \theta \\ b_1 \\ b_z \\ b_\theta \end{pmatrix}
\end{aligned}$$

The concepts defined in chapter 2 and chapter 3 are utilised together to develop this estimator. One can see how the characteristics of both TMF and LMF fit in the kind of desired estimation. The algebraic character of the mathematical relations of the estimation scheme and the recursivity between them allow to develop a simultaneous estimation.

Also, it is possible to use more complex equations (due to coupling in the vehicle dynamics) to estimate more parameters or states simultaneously, but this increases significantly the computational cost and the error increases. Coupled relations can be found in [SWSI13] and [Ell94].

5 Simulations

5.1 Model Considerations

Hereinafter, a 7DOF model is implemented for validation with no load transfer effect. The effect of the 7DOF that represent the handling model, i.e. the lateral and yaw motions are not considered. As input, a different road profile is defined for both right and left pair of wheels at constant speed as follows:

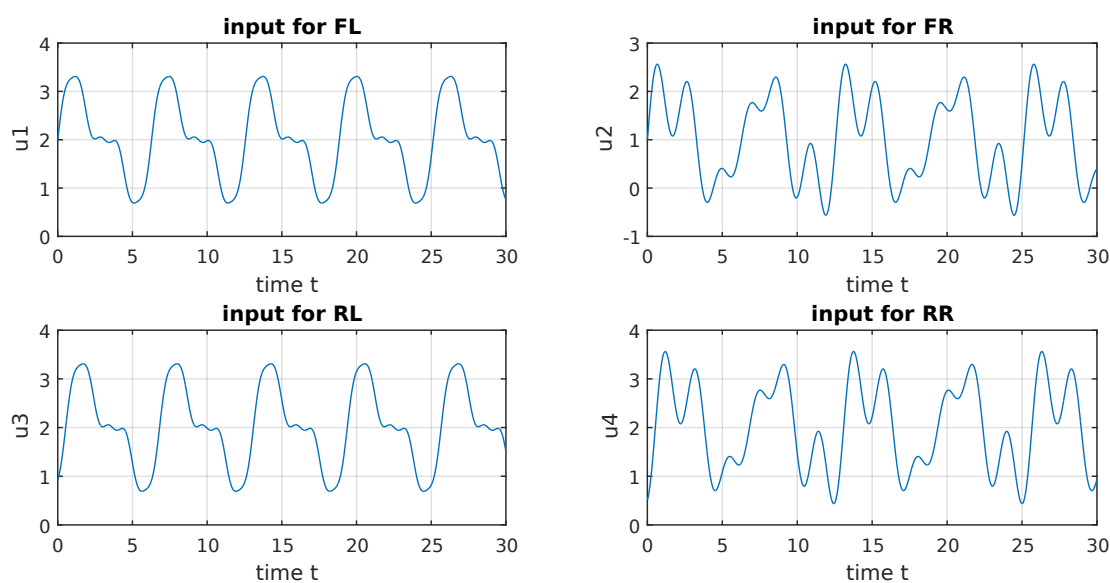


Figure 5.1: Road profile input

As can be seen above, a persistent excitation is considered in order to guarantee the convergence of the estimations. The significance of this element is explained in [Bes07].

5.2 Implementation

During the development of this work, MATLAB® and Simulink® were used for the implementation of the models and estimators. The model was developed in accordance

with the mathematical relations seen in Chapter 3.

The modulating functions were developed as a function in which one can freely choose the number of derivatives of the MF, the number of frequencies considered in the kernel, the time horizon and the desired type of MF with a structure according to chapter 2.2. For the inputs and the space-state representation of the model, a script was developed where the parameters (see Table 3.2) can be modified.

The implementation of the estimator is based on the implementation of an FIR filter in Simulink that has as input the readings of the sensors, and gives the respective Modulation Operator:

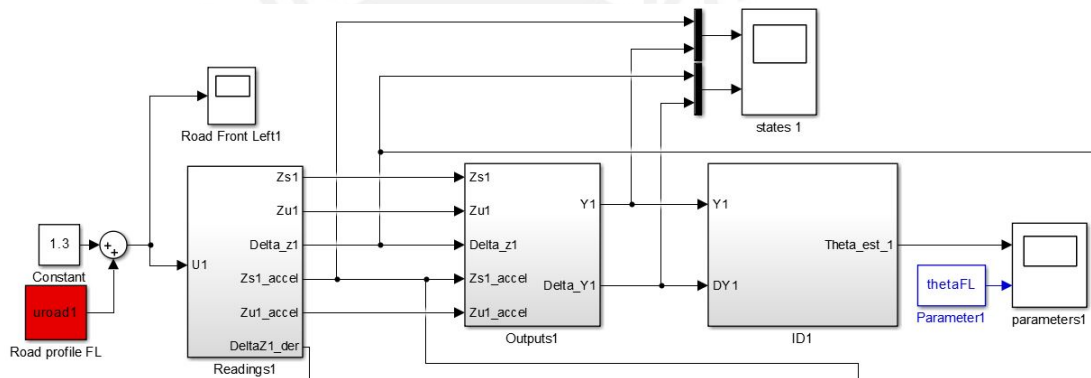


Figure 5.2: Estimator diagram

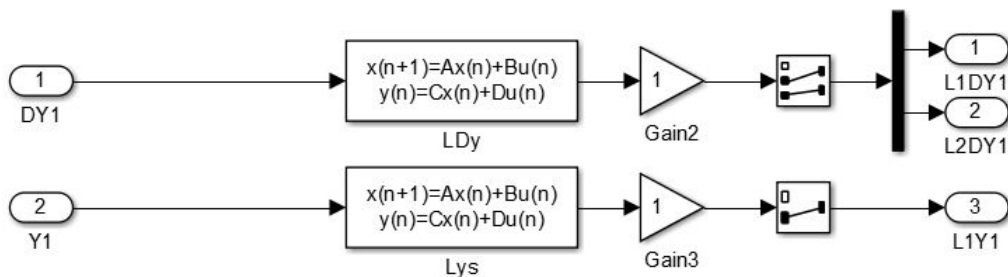


Figure 5.3: Modulation Operator

A sampling time of $10ms$ and ode4 (Runge-Kutta) as the solver are utilized during the simulations.

5.3 Analysis

First of all, a brief analysis with respect to the parameters of the MF is given. The following figure shows the TMF utilized during simulation:

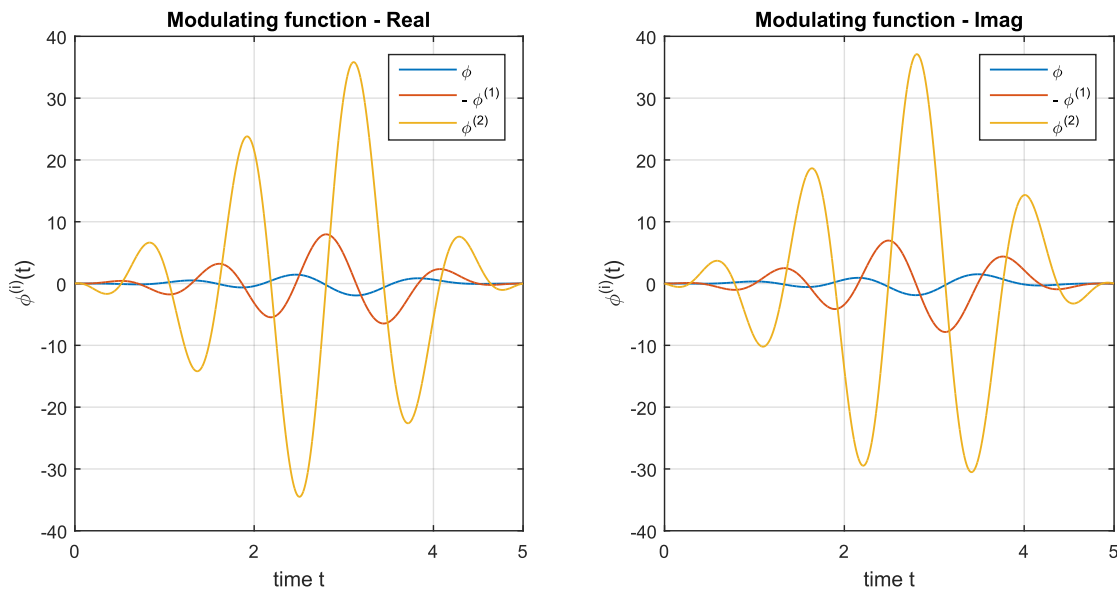


Figure 5.4: Total Modulation Function with $T=5$ and $N_w=5$

and now the same TMF if more frequencies are included, i.e N_w is higher:

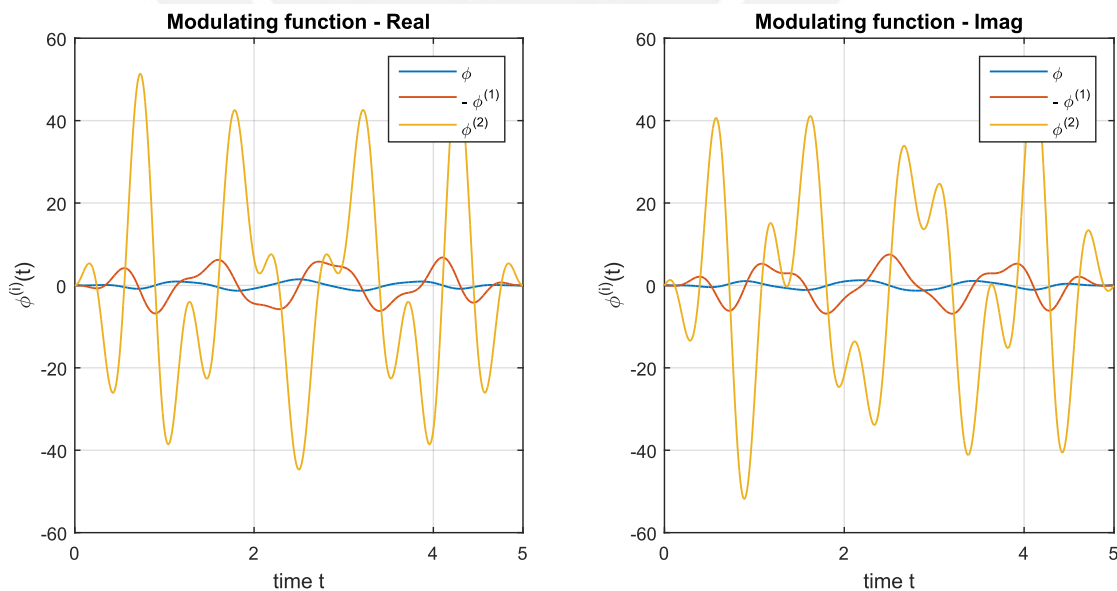


Figure 5.5: Total Modulation Function for $T=5$ and $N_w=10$

Up to this point, one can notice that the behaviour is similar. Now, considering the same number of frequencies, now is shown what happens if T is increased: One can no-

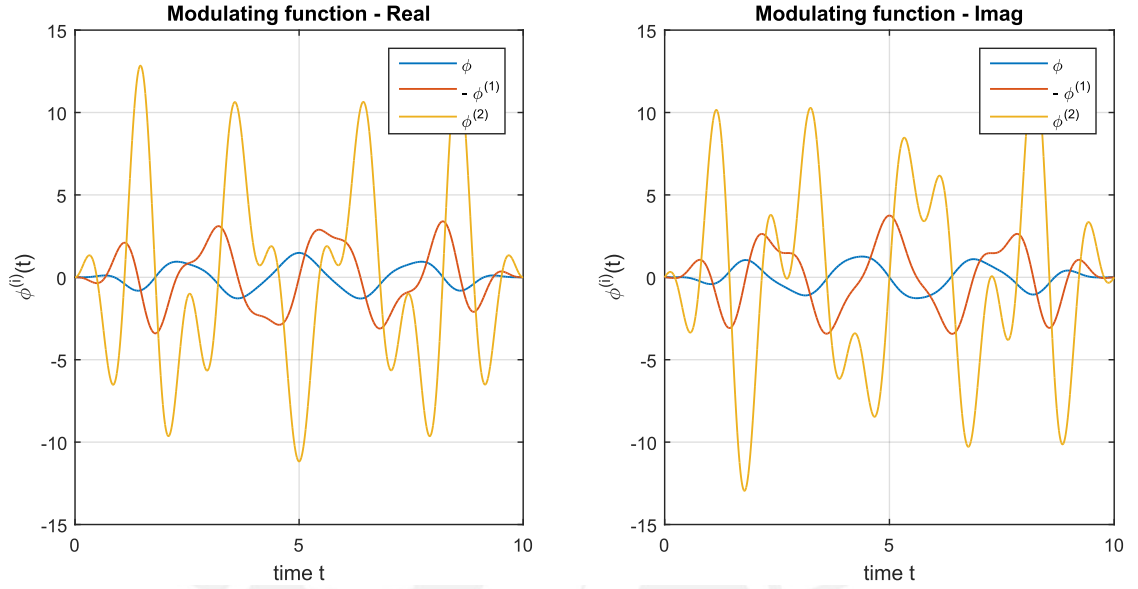
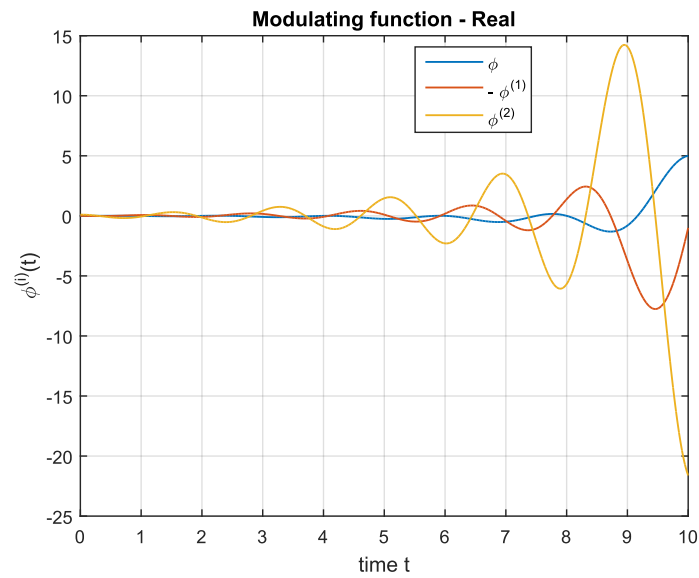


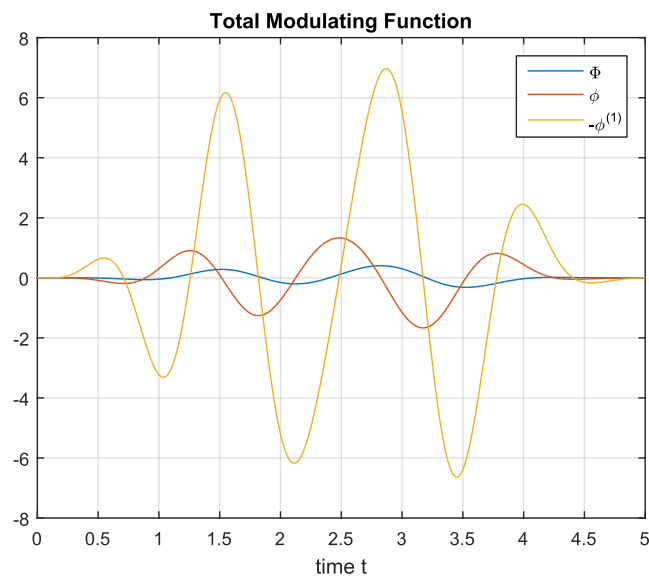
Figure 5.6: Total Modulation Function for $T=10$ and $N_w=10$

notice that the amplitude of φ and its derivatives are smaller when the horizon increases its value. On the one hand, this effect can be beneficial due to the minimization of numerical error. On the other hand, it increases the computational cost, which is not convenient for online estimation. It is important to consider that the estimation will be relevant after the time of the horizon T has elapsed. Choosing a horizon too small generates large deviation.

With respect to a LFM as a FDMF, figure (5.7) shows an example. As stated after (2.15), one can choose any derivative of the MF to multiply a signal, but one can notice that each derivative increases significantly the amplitude, what amplifies the error due to noise, so it is recommended to use the smaller that fits mathematically with the equations and what one want to estimate and neglect. The choice of N_ω also directly affects the estimation, as the derivatives of φ depend directly on $(j * \text{diag}(\omega))^i$, which increases the amplitude and causes the same issue.

Figure 5.7: Left Modulation Function for $T=10$ and $Nw=5$

Interestingly, the proposition made after (4.4) can be achieved, as $\Phi(0) = \Phi(T) = 0$:

Figure 5.8: Integral of $\varphi(t)$

So it is possible to reduce the derivative order by 1 if it can be proven that the properties of the Fourier MF are reflected on Φ .

Now, the outputs will be shown, so one can notice the effect of the measurement noise and the bias before the analysis of the estimations:

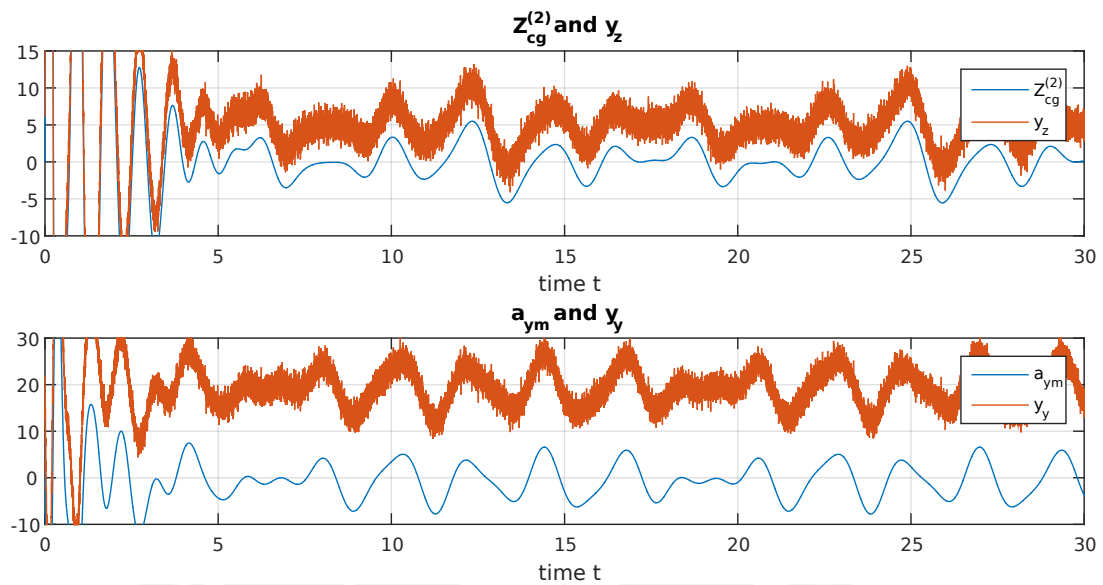


Figure 5.9: Vertical acceleration of COG

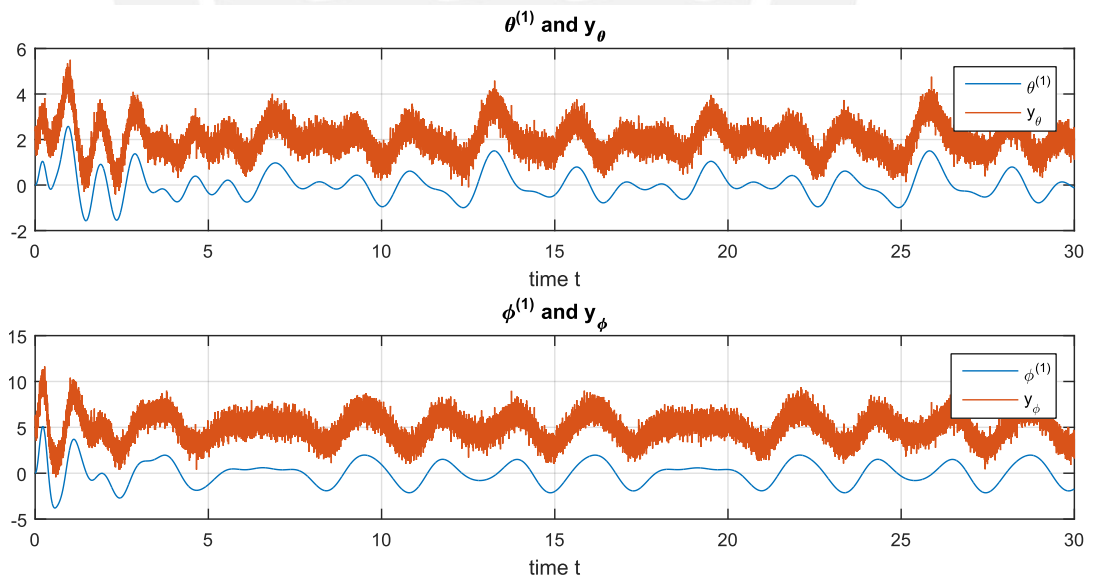


Figure 5.10: Pitch rate and Roll rate

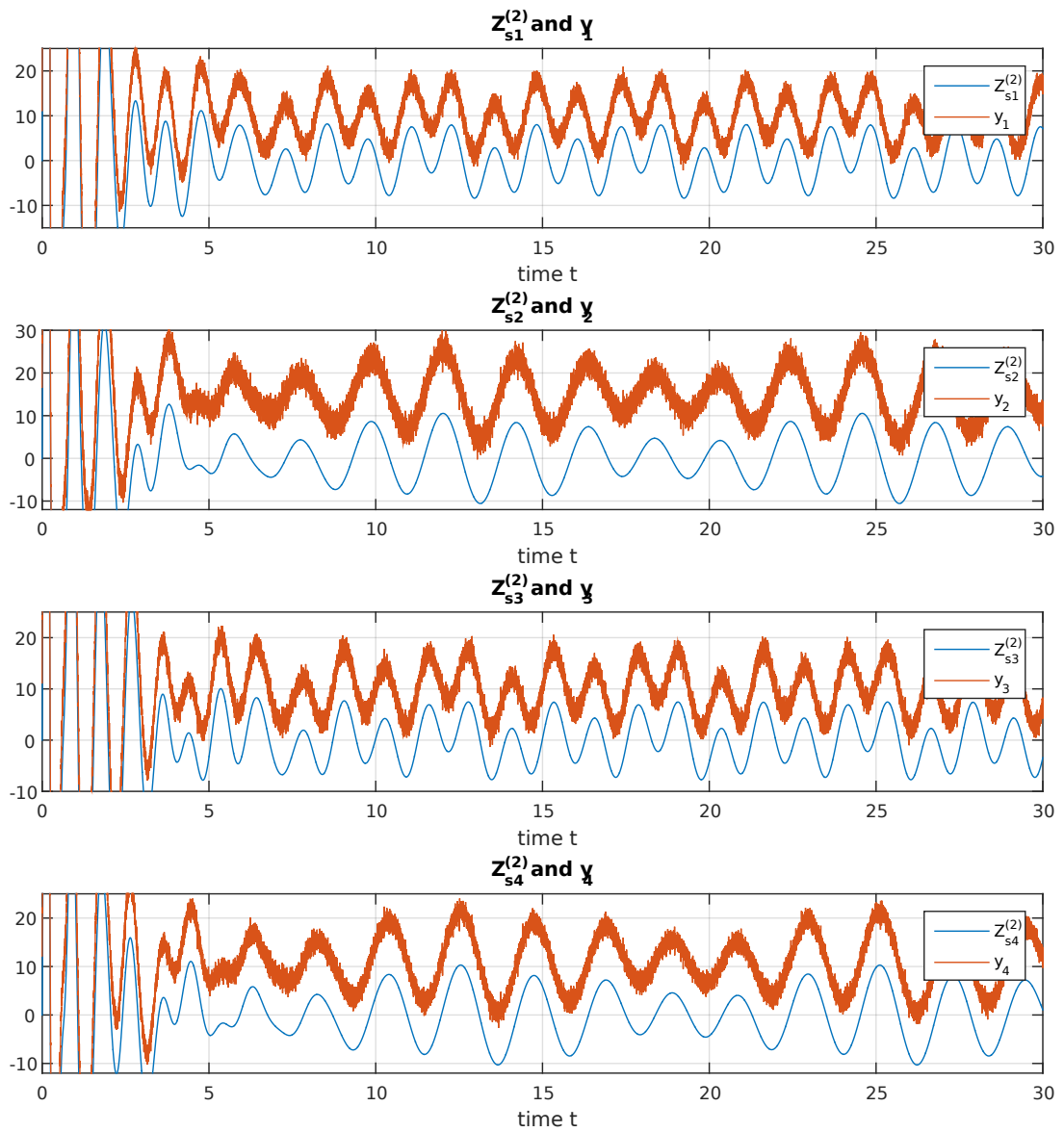


Figure 5.11: Vertical acceleration of sprung mass corners

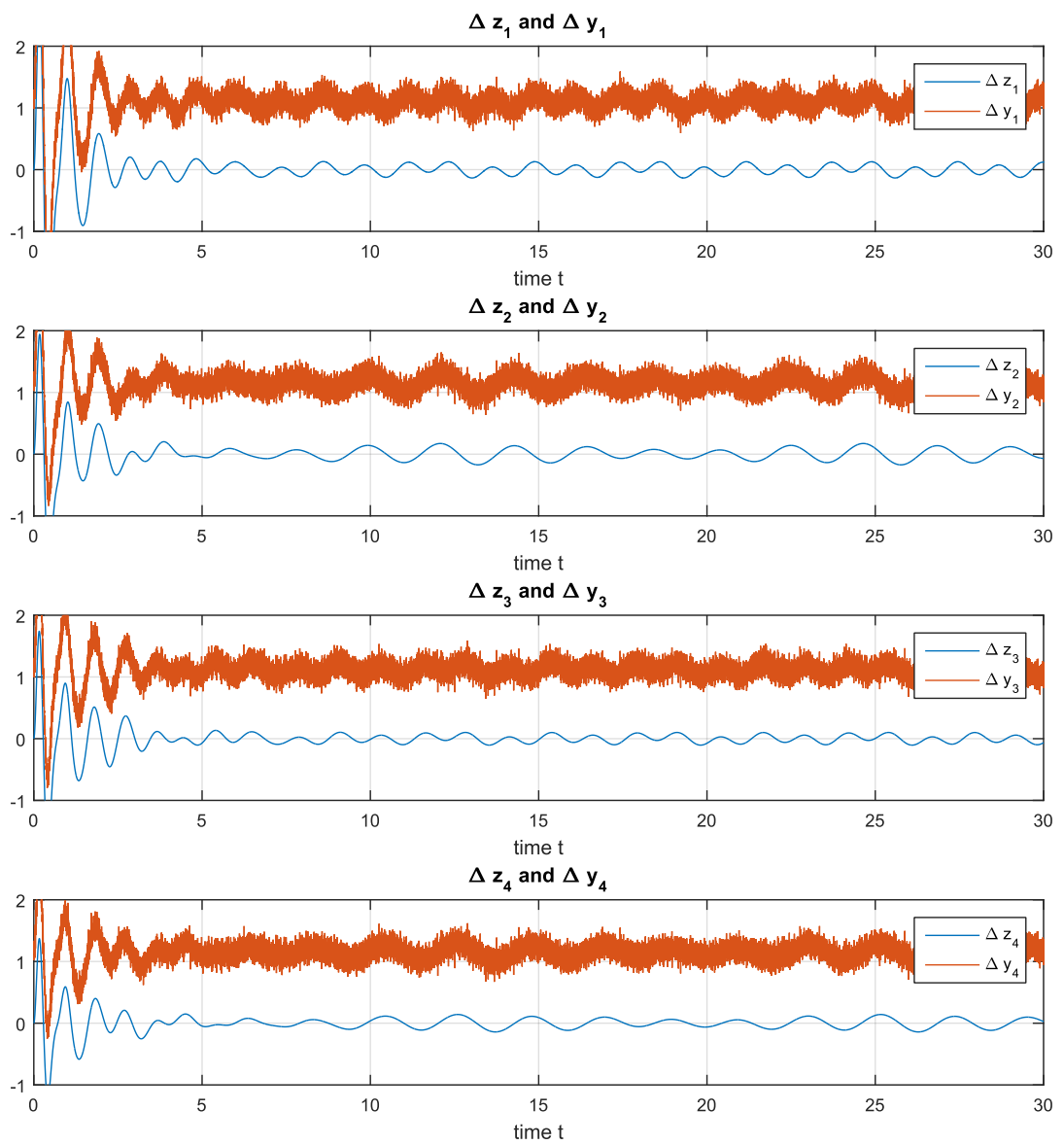


Figure 5.12: Suspension deflection sensors readings

For the analysis of the parameter estimation, the relations described in (4.4) are used. The MF described in figure 5.4 is utilized and gives:

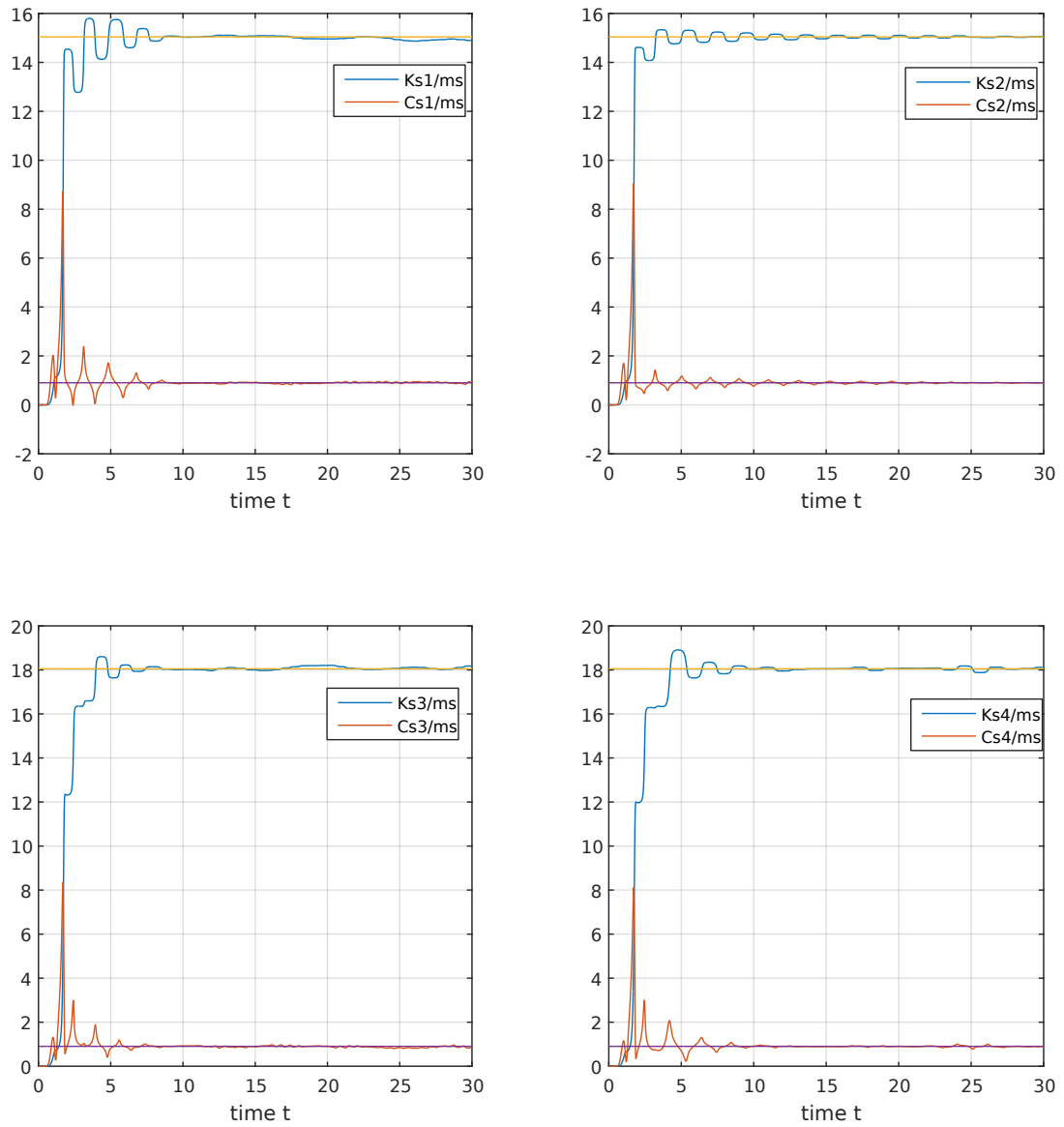


Figure 5.13: Estimated parameters for $T=5s$ and $N_w=5$

The error is represented by a Lyapunov function:

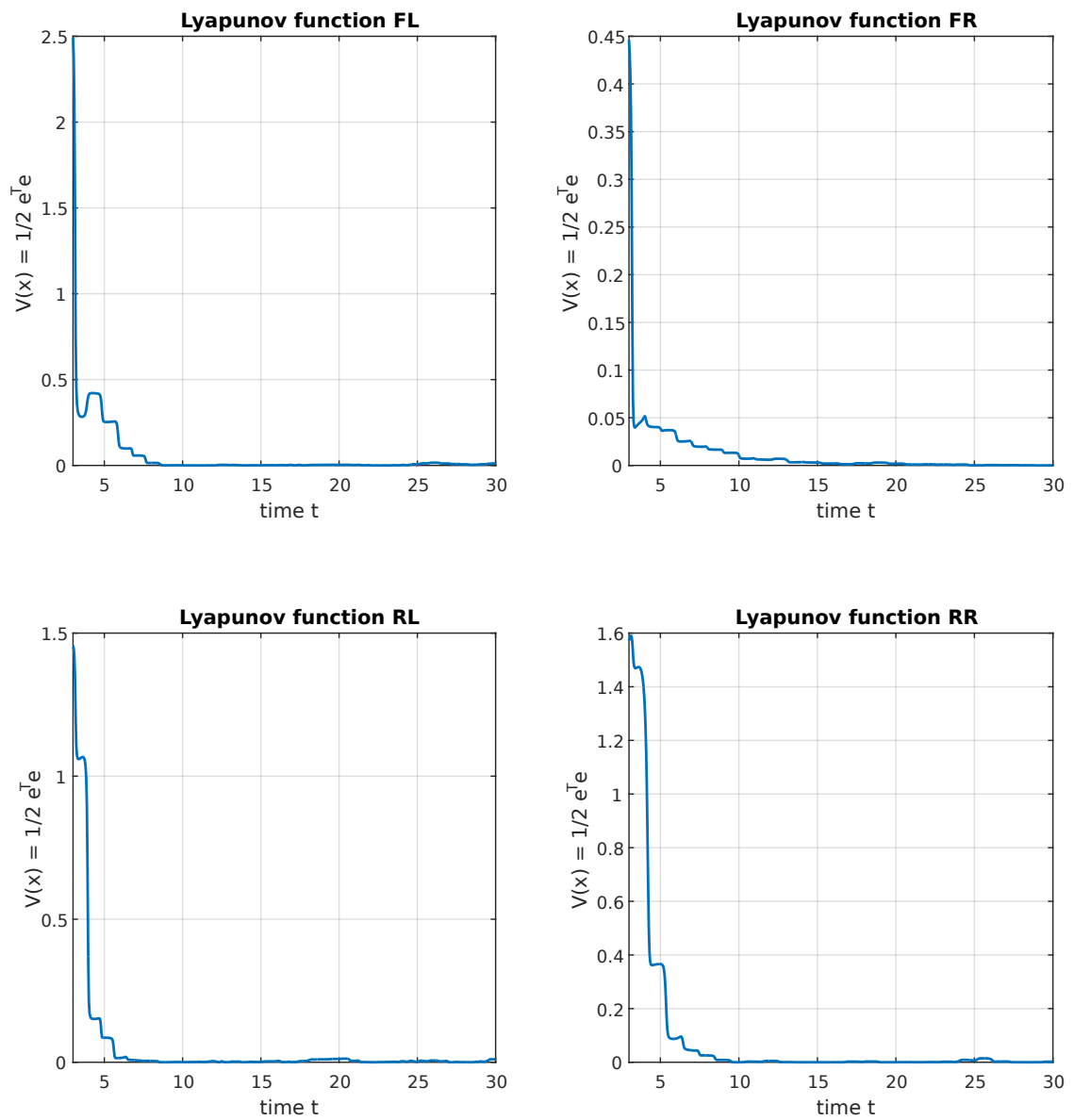


Figure 5.14: Error for $T=5s$ and $Nw=5$

A comparison with the estimation realized when the horizon $T = 10$ gives the following results:

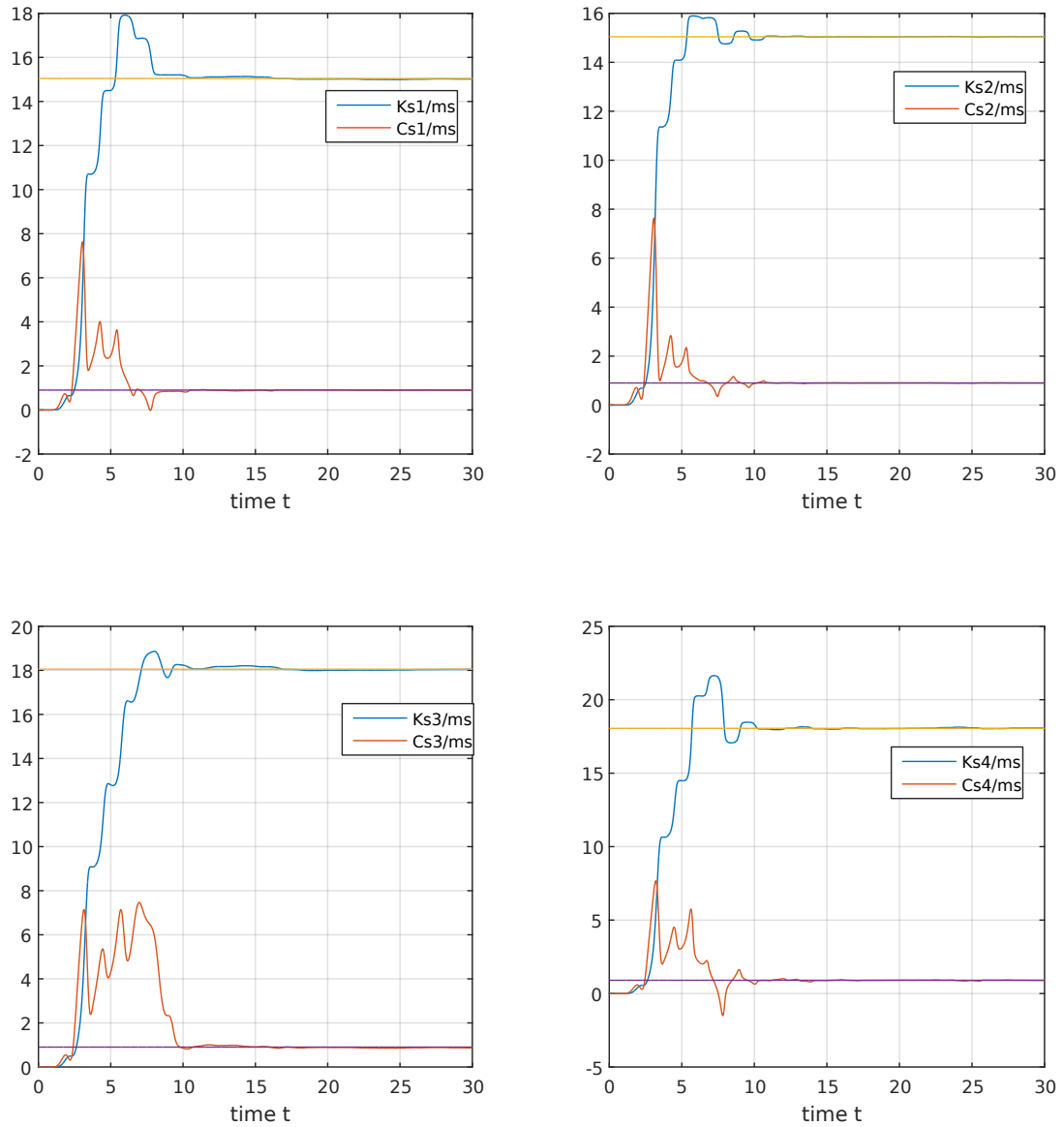
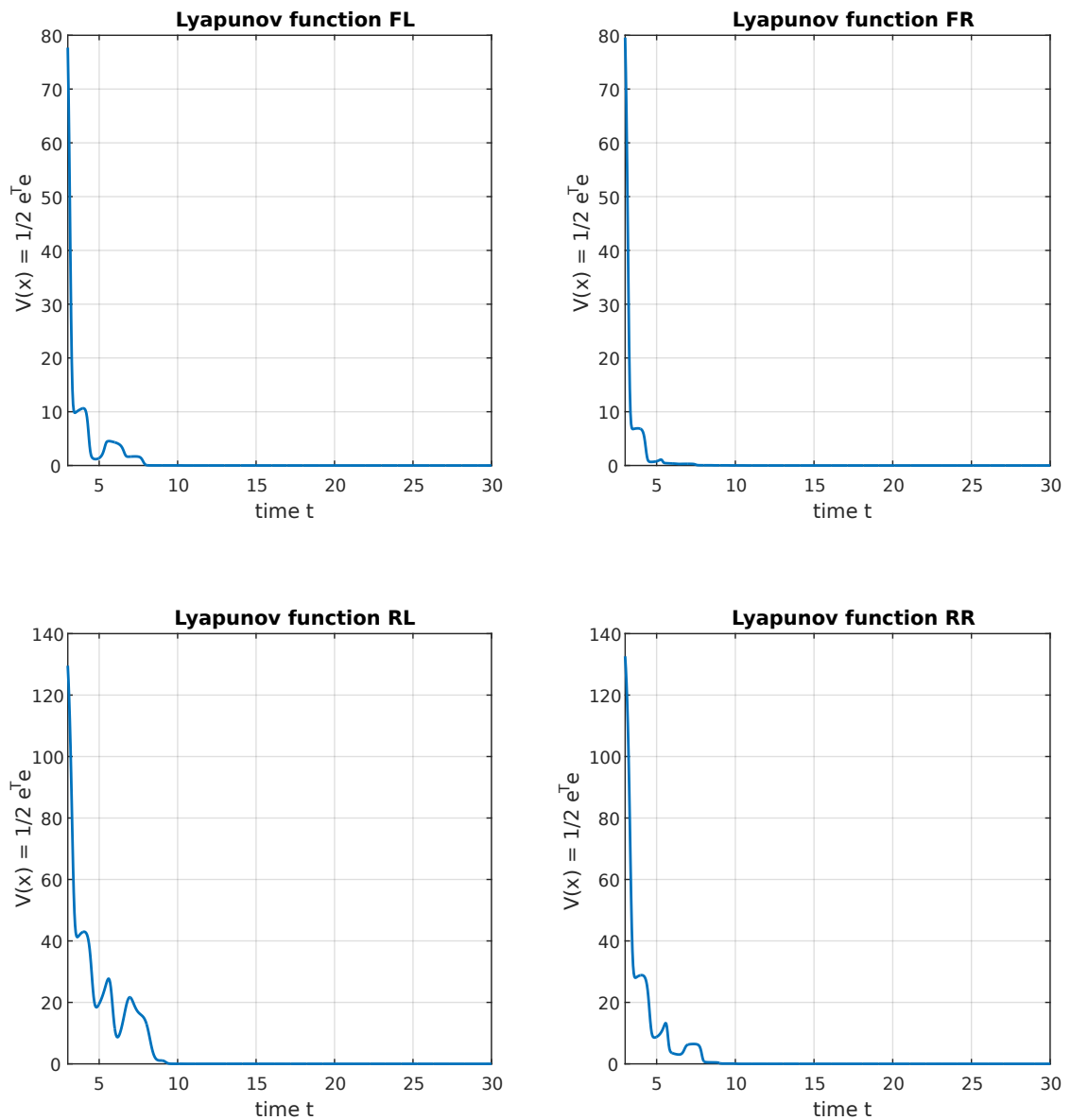


Figure 5.15: Estimated parameters for $T=10s$ and $Nw=5$

Figure 5.16: Error for $T=10$ s and $N_w=5$

One can notice that the estimation is more precise. This validates what was stated in the previous section. As was mentioned before, the estimation gives relevant information after the integration horizon has elapsed, that is the reason why the behaviour of the Lyapunov function is unexpected during the first T seconds. The small peaks after that time are consequence of the noisy sensor data.

Finally, the estimation of the roll angle ϕ is shown:

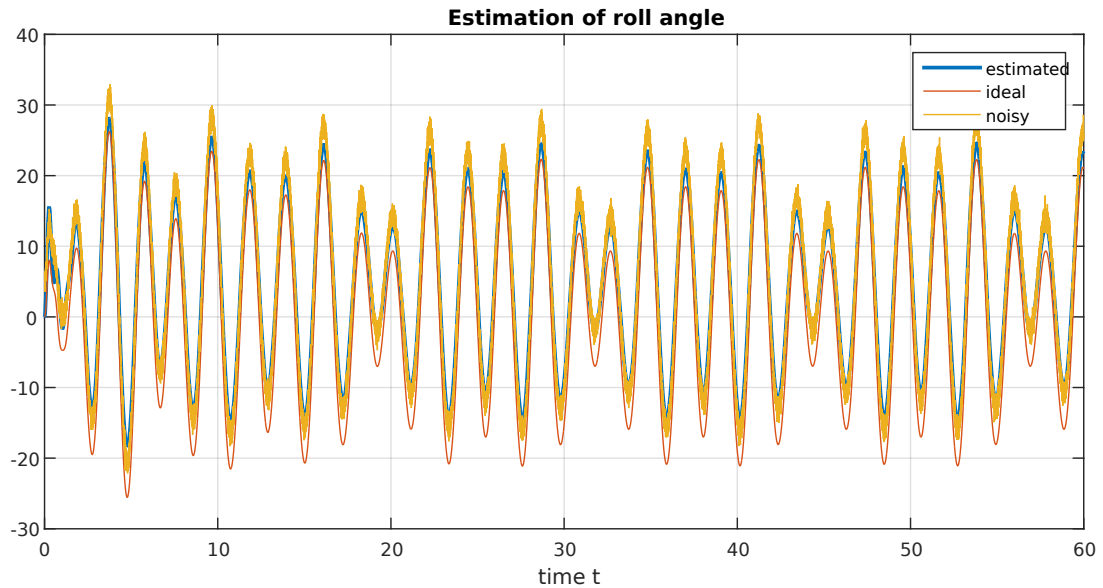


Figure 5.17: Roll angle estimation

It can be noticed that even for the big noise measurement seen in the reading of the sensors on figures 5.9 and 5.10, the estimation is really fast.

The parameters estimation can be realized online or offline, based on the dependence of the time varying parameters. For example, the vertical damping coefficient of a real vehicle has a non-linear behaviour when the deflection is too small, and varies when the suspension is compressed or stretched.

5.4 Comparison

Now, a Discrete Kalman Filter is implemented and the estimation is shown in Figure 5.18.

For this design, the bias is not compensated. Having the following State-Space representation:

$$\begin{aligned} \dot{x} &= f(x, u) \\ y &= h(x) + b \end{aligned} \quad (5.1)$$

And one can restructure it as follows:

$$\begin{aligned} \underbrace{\begin{pmatrix} \dot{x} \\ \dot{b} \end{pmatrix}}_{\dot{\tilde{x}}} &= \underbrace{\begin{pmatrix} f(x, u) & 0 \\ 0 & 0 \end{pmatrix}}_{\tilde{f}(\tilde{x})} \underbrace{\begin{pmatrix} x \\ b \end{pmatrix}}_{\tilde{x}} \\ y &= \underbrace{h(x) + b}_{\tilde{h}(\tilde{x})} \end{aligned} \quad (5.2)$$

so the bias is compensated.

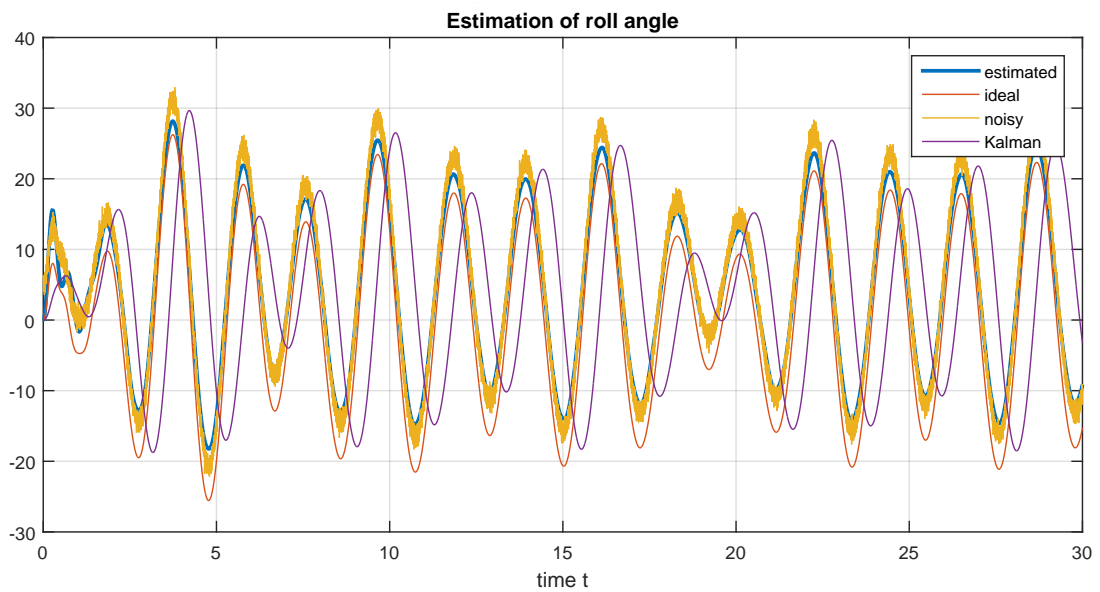


Figure 5.18: Comparison with Kalman Filter

A small phase lag can be noticed. This is inherent to low pass filtering. The frequency-domain properties that help to understand this behaviour are discussed in [GÅ87].

The developed observer shows a minimum phase lag and a more precise estimation.

6 Conclusions

Within the frame of this thesis, an on-line state estimator as well as a parameter identifier based on the FDMF have been developed for a terrestrial vehicle model. The results show that this approach is suitable for this kind of system. The noise and offsets implemented were exaggerated, but even the results gave a satisfactory robust estimation. As was stated at the beginning of this work, the idea of obtaining the desired information using cheap sensors seems feasible so far.

This work contributes developing an simultaneous estimation of parameters and states on a 4-wheel terrestrial vehicle. In [NBH⁺18], the time domain MF was utilised for a similar work with the assumption that the pitch and yaw are already known. This investigation uses the angular rate as the output of a real IMU. Also, here the frequency domain is utilised due to the properties of suppressing perturbing vibrations.

The implementation of an adaptive observer seems theoretically easy to design, but it can be noticed that many a more precise mathematical model will have more coupled relations between states and parameters, what increments the complexity. In this work, some assumptions were made, but on a real system, this will reduce reliance on the results. During the tests, some factors had to be considered such as choosing the best time horizon T and the number of frequencies N_ω , considering that incrementing or decreasing those values can bring better estimations, but increase the computational cost, as well as the simulation time. This approach gives good results on estimation while no higher derivatives of the MF φ are needed. Reducing the amplitude of this element only reduces the information carried during the modulation, and as a consequence, one gets more error during the estimation.

As a future work, the implementation of this method will be done with a full car model, and will be compared with the simultaneous estimator developed in [JR15]. Also, a comparison between this work and the estimation using Kalman Filtering stated in [DCVL12] and validated in [DCV12] will be interesting. The development

of an extended Kalman Filter to for the nonlinear behaviour of the full car model will allow a better comparison. Also, taking advantage of the properties of a full car model, it will be interesting to include encoders to read the velocities of the wheels, so the use of the MFT will allow to estimate the velocity of the car. Knowing the velocity can allow to decouple the mathematical relations that are used to estimate also the yaw angle.



List of Figures

1.1	Estimation scheme	3
3.1	14 DOF vehicle model	13
3.2	1 DOF vehicle model	15
4.1	Sensors configuration	17
4.2	Example of initial condition of suspension deflection sensors	20
5.1	Road profile input	23
5.2	Estimator diagram	24
5.3	Modulation Operator	24
5.4	Total Modulation Function with $T=5$ and $Nw=5$	25
5.5	Total Modulation Function for $T=5$ and $Nw=10$	25
5.6	Total Modulation Function for $T=10$ and $Nw=10$	26
5.7	Left Modulation Function for $T=10$ and $Nw=5$	27
5.8	Integral of $\varphi(t)$	27
5.9	Vertical acceleration of COG	28
5.10	Pitch rate and Roll rate	28
5.11	Vertical acceleration of sprung mass corners	29
5.12	Suspension deflection sensors readings	30
5.13	Estimated parameters for $T=5s$ and $Nw=5$	31
5.14	Error for $T=5s$ and $Nw=5$	32
5.15	Estimated parameters for $T=10s$ and $Nw=5$	33
5.16	Error for $T=10s$ and $Nw=5$	34
5.17	Roll angle estimation	35
5.18	Comparison with Kalman Filter	36

List of Tables

3.1	Described variables	15
3.2	Technical parameters	16



Bibliography

- [Agu14] AGUIRRE, Oscar Benjamin C.: *Systems Identification Using Fourier And Hartley Modulation Functions*, Technische Universität Ilmenau, Diplomarbeit, März 2014
- [ART14] AGUIRRE, Oscar C. ; REGER, Johann ; TAFUR, Julio: Frequency domain modulating functions for continuous-time identification of linear and nonlinear systems 16th Latinamerican Control Conference (CLCA 2014), 2014, S. 394 — 399
- [Bes07] *Kapitel 1*. In: BESANÇON, G.: *An overview on observer tools for nonlinear systems*. 2007, S. 1–33
- [DCV12] DOUMIATI, M. ; CHARARA, A. ; VICTORINO, A.: *Vehicle Dynamics Estimation Using Kalman Filtering: Experimental Validation*. ISTE LTD, 2012
- [DCVL12] DOUMIATI, Moustapha ; CHARARA, Ali ; VICTORINO, Alessandro ; LECHNER, Daniel: *Vehicle Dynamics Estimation using Kalman Filtering*. John Wiley & Sons, 2012 https://www.ebook.de/de/product/21167934/moustapha_doumiati_ali_charara_alessandro_victorino_daniel_lechner_vehicle_dynamics_estimation_using_kalman_filtering.html
- [Ell94] ELLIS, J. R. ; LIMITED, Mechanical Engineering P. (Hrsg.): *Vehicle Handling Dynamics*. Page Bros, 1994
- [GÅ87] GRIMBLE, M. J. ; ÅSTRÖM, K. J.: Frequency-domain properties of Kalman filters. In: *International Journal of Control* 45 (1987), mar, Nr. 3, S. 907–925. <http://dx.doi.org/10.1080/00207178708933777>. – DOI 10.1080/00207178708933777

- [HBM04] HAC, Aleksander ; BROWN, Todd ; MARTENS, John: Detection of Vehicle Rollover. In: *SAE Technical Paper Series* 01 (2004), März, Nr. 1575
- [JR15] JOUFFROY, Jerome ; REGER, Johann: Finite-time simultaneous parameter and state estimation using modulating functions 2015 IEEE Conference on Control Applications (CCA 2015), 2015, S. 394–399
- [NBH⁺18] NOACK, Matti ; BOTHA, Theunis ; HERMAN, A. ; HAMERSMA ; IVANOV, Valentin ; REGER, Johann ; ELS, Schalk: Road profile estimation with modulation function based sensor fusion and series expansion for input reconstruction. (2018), März
- [NPL⁺18] NA, Wonbin ; PARK, Changwoo ; LEE, Seokjoo ; YU, Seongo ; LEE, Hyeongcheol: Sensitivity-Based Fault Detection and Isolation Algorithm for Road Vehicle Chassis Sensors. In: *Sensors* 18 (2018), Nr. 8
- [NRERM16] NOACK, M. ; RUEDA-ESCOBEDO, J. G. ; REGER, J. ; MORENO, J. A.: Fixedtime parameter estimation in polynomial systems through modulating functions. In: *Proceedings of the 55th IEEE Conference on Decision and Control* (2016), Dezember, S. 2067–2072
- [PL85] PEARSON, A. E. ; LEE, F.: On the identification of polynomial input-output differential systems. In: *IEEE Transactions on Automatic Control* 30 (1985), Nr. 8
- [Shi57] SHINBROT, Marvin: On the analysis of linear and nonlinear systems. In: *Transactions of ASME* Bd. 79, 1957, S. 547–552
- [SSS09] SETIAWAN, Joga D. ; SAFARUDIN, Mochamad ; SINGH, Amrik: *Modeling, Simulation and Validation of 14 DOF Full Vehicle Model*, Diponegoro University and University Teknikal Malaysia Melaka, Diplomarbeit, 2009
- [SWSI13] SHYROKAU, B. ; WANG, D. ; SAVITSKI, D. ; IVANOV, V.: Vehicle dynamics control with energy recuperation based on control allocation for independent wheel motors and brake system. In: *International Journal of Powertrains* 2 (2013), Januar, Nr. 2/3, S. 153
- [Web17] WEBER, Markus: *Zustandsschätzung mittels Modulationsfunktionen auf Grundlage von Frequenzbereichsbetrachtungen*, Technische Universität Ilmenau, Diplomarbeit, Juli 2017